BIOCHEMISTRY

Cla4 phosphorylates histone methyltransferase Set1 to prevent its degradation by the APC/C^{Cdh1} complex

Xuanyunjing Gong[1]†, Shanshan Wang[1]†, Qi Yu[1], Min Wang[2], Feng Ge[2], Shanshan Li[1]*, Xilan Yu[1]*

H3K4 trimethylation (H3K4me3) is a conserved histone modification catalyzed by histone methyltransferase Set1, and its dysregulation is associated with pathologies. Here, we show that Set1 is intrinsically unstable and elucidate how its protein levels are controlled within cell cycle and during gene transcription. Specifically, Set1 contains a destruction box (D-box) that is recognized by E3 ligase APC/C^{Cdh1} and degraded by the ubiquitin-proteasome pathway. Cla4 phosphorylates serine 228 (S228) within Set1 D-box, which inhibits APC/C^{Cdh1}-mediated Set1 proteolysis. During gene transcription, PAF complex facilitates Cla4 to phosphorylate Set1-S228 and protect chromatin-bound Set1 from degradation. By modulating Set1 stability and its binding to chromatin, Cla4 and APC/C^{Cdh1} control H3K4me3 levels, which then regulate gene transcription, cell cycle progression, and chronological aging. In addition, there are 141 proteins containing the D-box that can be potentially phosphorylated by Cla4 to prevent their degradation by APC/C^{Cdh1}. We addressed the long-standing question about how Set1 stability is controlled and uncovered a new mechanism to regulate protein stability.

INTRODUCTION

The eukaryotic DNA is present as a chromatin structure within the nucleus. Two copies each of core histones (H2A, H2B, H3, and H4) form an octamer, which is wrapped by ~147 base pairs (bp) of DNA to form a nucleosome. Together with the linker histone H1, nucleosomes can adopt different levels of compaction to form chromatin. The highly conserved histone proteins undergo several types of posttranslational modifications including acetylation, methylation, phosphorylation, and ubiquitylation. These histone modifications are deposited or removed by specific chromatin-modifying enzymes, which could alter chromatin structure and/or form a platform to recruit other factors to regulate gene transcription, DNA replication, and repair, and are involved in processes that determine cell fate and development (*1*, *2*). The expression of these chromatin-modifying enzymes needs to be tightly controlled to establish and maintain proper chromatin modifications, and their dysregulation may lead to diseases, i.e., cancer and development defects (*3*–*7*).

H3 lysine 4 trimethylation (H3K4me3) is a highly conserved histone modification that plays important roles in gene transcription, DNA repair, and class-switch recombination (*8*–*10*). The mutation of H3K4 to methionine (H3K4M) has been found in several cancer types, and defects in histone H3K4 methylation are associated with diverse pathologies such as acute myeloid leukemia (AML) (*8*, *11*, *12*), emphasizing the importance of studying H3K4me3 regulatory pathways. H3K4 methylation is catalyzed by an evolutionarily conserved family of methyltransferases referred to as the complex of proteins associated with Set1 (COMPASS). In humans, H3K4 methylation is catalyzed by the SET1/mixed lineage leukemia (MLL) family of histone methyltransferases (HMTs), which consists of six family members, MLL1 to MLL4, SET1A, and SET1B. In budding yeast, H3K4 methylation is catalyzed by the sole HMT, Set1, which serves as an excellent model to study multiple SET1/MLL family members in higher organisms. Set1 and its homologs in other organisms are associated with additional proteins that regulate its HMT activity. Set1 is present in the COMPASS complex that is composed of the catalytic subunit (Set1) and seven other subunits (Swd1, Swd2, Swd3, Bre2, Sdc1, Spp1, and Shg1) (*8*). During early gene transcription process, the COMPASS complex is recruited to 5′ end of genes. This process requires the C-terminal domain (CTD) of RNA polymerase II (RNA Pol II) phosphorylated at the serine 5 (Ser^5) of its heptad repeats as well as the presence of the RNA Pol II–associated factor (PAF) complex (*13*, *14*). The PAF complex consists of five subunits (Paf1, Ctr9, Leo1, Rtf1, and Cdc73) (*15*). The PAF complex facilitates the recruitment of COMPASS complex to ensure the proper distribution of H3K4 methylation on chromatin (*13*, *14*).

The expression of Set1 is important to establish and maintain proper levels of H3K4 methylation. Set1 expression is regulated by 13 histone substitution mutations (*16*). In particular, Gcn5-catalyzed H3K14 acetylation promotes the transcription of *SET1* to maintain normal levels of H3K4me3 (*16*). Loss of H3K4 methyltransferase activity leads to reduced Set1 protein levels (*17*). In addition, the PAF complex is required for the binding of Set1 with chromatin, which also stabilizes Set1 (*17*). Although deletion of the N-terminal 780 amino acids of Set1 has been shown to stabilize Set1 (*17*), it remains unknown about the underlying mechanism.

We have previously reported that Set1-catalyzed H3K4me3 promotes the transcription of four core histones and maintains normal chronological life span (*18*, *19*). As the transcription of core histones is tightly controlled by the cell cycle with their transcription peaked at S phase (*18*, *20*), we wondered whether the Set1 protein levels are regulated by the cell cycle. Set1 levels oscillate within the cell cycle: They were very low in G_1 phase, but gradually increased in S phase and peaked in G_2-M phase. Mechanistically, we identified a destruction box (D-box) within Set1 N terminus that enables Set1 to be degraded by Cdh1 within the anaphase-promoting complex/cyclosome (APC/C ^{Cdh1}) complex. The p21-activated kinase (PAK) Cla4

[1]State Key Laboratory of Biocatalysis and Enzyme Engineering, National & Local Joint Engineering Research Center of High-throughput Drug Screening Technology, School of Life Sciences, Hubei University, Wuhan, Hubei 430062, China. [2]Key Laboratory of Algal Biology, Institute of Hydrobiology, Chinese Academy of Sciences, Wuhan, Hubei 430072, China.
*Corresponding author. Email: shl@hubu.edu.cn (S.L.); yuxilan@hubu.edu.cn (X.Y.)
†These authors contributed equally to this work.

phosphorylates serine 228 (S228) within the D-box of Set1, preventing it from being recognized and degraded by the E3 ligase APC/C^{Cdh1} complex. Cla4-catalyzed Set1-S228 phosphorylation is enhanced by the PAF complex to stabilize Set1 during gene transcription. Moreover, Cla4-catalyzed Set1-S228 phosphorylation enhances Set1-catalyzed H3K4me3, which promotes gene transcription, maintains telomere silencing, and extends chronological life span. By applying bioinformatics and proteomics tools, we identified a total of 141 yeast proteins containing D-box that can be potentially phosphorylated by Cla4 to prevent their degradation mediated by the APC/C^{Cdh1} complex. Our work not only addressed how Set1 stability is controlled but also revealed a mechanism to regulate protein stability by Cla4 and the APC/C^{Cdh1} complex.

RESULTS

Set1 protein levels fluctuate throughout the cell cycle

To assess the expression of Set1 over the cell cycle, yeast cells were first synchronized at G_1 phase by α-factor. After α-factor release, samples were taken every 15 min over a 2-hour time course and processed for fluorescence-activated cell sorting (FACS) analysis and immunoblot analysis. The intracellular Set1 protein levels were lowest in G_1 phase and gradually increased toward S and G_2 (Fig. 1A). In contrast with this marked difference in protein levels, the *SET1* mRNA levels changed less than 1.5-fold throughout the cell cycle (fig. S1A). We individually synchronized cells at G_1 phase with α-factor, S phase with hydroxyurea (HU), and G_2-M phase with nocodazole (Noco). In these synchronized cells, the abundance of Set1 was still lowest in G_1 phase (Fig. 1B). This G_1 depletion is specific to Set1 as the levels of other HMTs, Set2 and Dot1, remained constant throughout the cell cycle (Fig. 1B).

There are two major systems to regulate protein turnover in eukaryotic cells: the ubiquitin-proteasome pathway and autophagy (*21*). To characterize the mechanism responsible for Set1 degradation in G_1, we synchronized cells in G_1 with α-factor and then treated cells with the proteasome inhibitor MG132, or the inhibitor for lysosomal proteases phenylmethylsulfonyl fluoride (PMSF) (*22*). In G_1-arrested cells, the endogenous Set1 was significantly increased by MG132 but not PMSF treatment (Fig. 1C). The Set1 protein levels were also significantly increased in a temperature-sensitive proteasome-deficient strain (*cim3-1*) at a nonpermissive temperature (37°C) (fig. S1B). These results indicate that Set1 is specifically degraded in G_1 phase by the ubiquitin-proteasome pathway.

The APC/C^{Cdh1} complex mediates Set1 polyubiquitination and degradation

To explore the mechanism for Set1 degradation, we first attempted to identify the E3 ubiquitin ligase. It has been reported that deletion of the N-terminal 780 amino acids of Set1 (Set1 780Δ) increased the global Set1 protein levels (*17*). We constructed the Set1 780Δ mutant and observed that loss of the N-terminal 780 residues (Set1 780Δ) markedly increased the intracellular Set1 levels (fig. S1C), suggesting that the N-terminal 780 amino acids of Set1 contain a degron sequence. By analyzing the N-terminal region of Set1, we found that the sequence $_{226}$RNSL$_{229}$ conforms the consensus sequence (RXXL) of the destruction box (D-box) that can be recognized by Cdh1 and Cdc20, the adaptors for the anaphase-promoting complex/cyclosome (APC/C) complex (Fig. 1D) (*23*, *24*). The APC/C complex is a multi-subunit E3 ubiquitin ligase that mediates the polyubiquitination of its target proteins, which are then degraded by the 26S proteasome (*25*). Cdh1 and Cdc20 act as the adaptor proteins that bring substrates to the APC/C complex. We thus mutated the D-box sequence (RNSL) within Set1 to KNSA (Set1-KNSA) (Fig. 1D). The protein levels of endogenous Set1-KNSA mutant were significantly higher than those of wild type (WT) Set1 (Fig. 1E). When WT Set1 and Set1-KNSA cells were arrested in G_1 phase with α-factor and then treated with cycloheximide (CHX) to inhibit new protein synthesis, Set1 was gradually lost especially 40 min after translation shutoff but the Set1 protein levels in Set1-KNSA mutant remained constantly higher and its half-life was markedly extended (fig. S1D).

The above data showed that Set1 N-terminal domain contains a D-box that makes it unstable. As D-box can be recognized by Cdh1 and Cdc20, the adaptors for the APC/C complex (*23*, *24*), we then determined whether the APC/C complex is required for Set1 degradation. Deletion of APC/C complex subunits *APC10* and *APC13* significantly increased Set1 protein levels (fig. S1E). The APC/C adaptor proteins Cdh1 and Cdc20 contribute to APC/C substrate recognition by binding to the degron sequence within the target proteins (*23*). Loss of Cdh1, but not Cdc20, remarkably increased Set1 protein levels, and overexpression of *CDH1* reduced Set1 protein levels (Fig. 1F and fig. S1E), indicating that the APC/C^{Cdh1} complex is responsible for Set1 degradation. We also synchronized WT and *cdh1*Δ mutant at G_1, S, and G_2-M phases with α-factor, HU, and Noco, respectively. The intracellular Set1 levels in *cdh1*Δ mutant were substantially increased in G_1 and slightly increased in G_2-M (Fig. 1G), suggesting that Cdh1 initiates Set1 degradation in G_1 and modest degradation in G_2-M. Moreover, loss of Cdh1 or mutation of Set1-KNSA reduced the ubiquitination level of Set1 (Fig. 1H). To directly show that Cdh1 mediates the polyubiquitination of Set1, we performed an in vitro ubiquitination assay with purified Set1 and Cdh1. In the presence of purified ubiquitin-activating enzyme Ube1 (E1) and ubiquitin-conjugating enzyme Ubc4 (E2), Cdh1 (E3) is able to catalyze Set1 polyubiquitination as indicated by the accumulation of high molecular weight species (Fig. 1I).

To show that Cdh1 recognizes the D-box sequence on Set1, we performed the co-immunoprecipitation (Co-IP) assay and observed that Cdh1 interacted with Set1 (Fig. 1, J and K). We also performed the in vitro Co-IP by immobilizing WT FLAG-Set1 and FLAG-Set1-KNSA mutant on anti-FLAG beads and then incubating them with purified recombinant Cdh1. Set1-KNSA mutant showed reduced interaction with Cdh1 when compared with WT Set1 (Fig. 1L, lane 3 versus lane 4). The remaining weak interaction between Cdh1 and Set1-KNSA suggests that other domains of Set1 may also contribute to the interaction between Set1 and Cdh1. Therefore, we identified the APC/C^{Cdh1} complex as the E3 ligase that recognizes the Set1 D-box sequence and triggers Set1 degradation in G_1 phase and modest turnover in early mitosis.

Cla4 phosphorylates Set1 at S228 to stabilize Set1

When we analyzed the N-terminal region of Set1, we found that S228 within the D-box (RNS228L) of Set1 was predicted to be phosphorylated (group-based prediction system). To determine whether Set1 was phosphorylated at S228, we generated an antibody (anti–Set1-S228p) that recognizes Set1-S228 phosphorylation with high specificity (fig. S2A). Using this anti–Set1-S228p antibody, we

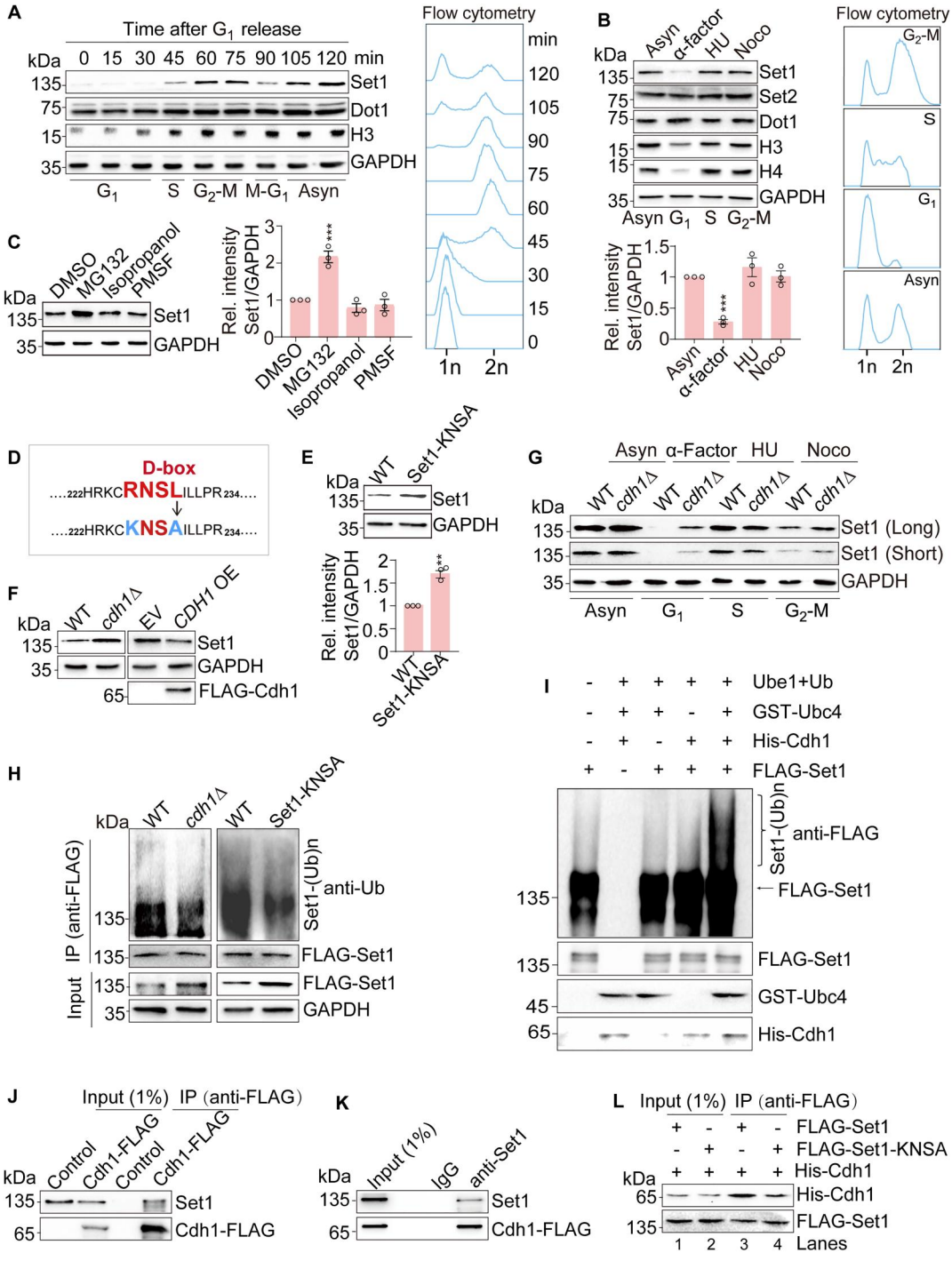

Fig. 1. Set1 is degraded by the APC/C^{Cdh1} complex. (**A**) Set1 protein levels were cell cycle regulated. Yeast cells were arrested in G_1 phase using α-factor for 3 hours and then released into fresh YPD medium. Cells were harvested at indicated time points and then subjected to immunoblot analysis (left panel) and flow cytometry analysis (right panel). (**B**) Set1 protein levels were reduced in G_1 phase. Cells were arrested in G_1, S, and G_2-M using α-factor (10 μg/ml), 10 μM HU, and 8 μM nocodazole (Noco) for 3 hours, respectively. (**C**) Immunoblot analysis of Set1 in cells treated with 5 mM MG132 or 5 mM PMSF for 2 hours. Cells were treated with dimethyl sulfoxide (DMSO) and isopropanol as controls. (**D**) Diagram showing the D-box (226-RNSL-229) within WT Set1 and mutated D-box (226-KNSA-229) within Set1-KNSA mutant. (**E**) Immunoblot analysis of Set1 in WT and Set1-KNSA mutant. (**F**) Immunoblot analysis of Set1 in WT, *cdh1*Δ, and Cdh1 overexpression (*CDH1* OE) cells. Cells transfected with empty vector (EV) were used as controls. (**G**) Immunoblot analysis of Set1 in WT and *cdh1*Δ mutant synchronized at G_1, S, and G_2-M phases by α-factor, HU, or Noco for 3 hours, respectively. (**H**) Analysis of Set1 ubiquitination in WT, *cdh1*Δ, and Set1-KNSA mutants. (**I**) In vitro ubiquitination assay showing that Cdh1 can mediate Set1 polyubiquitination. (**J** and **K**) Set1 interacted with Cdh1 as determined by Co-IP and reciprocal IP. Cells expressing untagged endogenous Cdh1 were used as a negative control. (**L**) In vitro Co-IP showing that Cdh1 preferentially bound WT Set1 but not Set1-KNSA mutant. The purified FLAG-Set1 and FLAG-Set1-KNSA were incubated with the purified recombinant His-Cdh1. Set1 was immunoprecipitated with anti-FLAG agarose. For (B), (C), and (E), data represent the mean ± SE of three biological independent experiments. *P < 0.05, **P < 0.01, ***P < 0.001.

detected the intracellular Set1-S228 phosphorylation in endogenously expressed WT but not in endogenously expressed nonphosphorylatable Set1-S228A mutant (Fig. 2A). The immunofluorescence assay revealed that Set1-S228 phosphorylation mainly occurred in the nucleus (fig. S2B). All these data indicate that Set1 can be phosphorylated at S228.

We then examined the effect of Set1-S228 phosphorylation on Set1 expression levels. Although the transcription of *SET1* was not significantly altered in endogenously expressed nonphosphorylatable Set1-S228A mutant and phosphomimetic Set1-S228E mutant (fig. S2C), mutation of Set1-S228A significantly reduced Set1 protein levels and mutation of Set1-S228E increased Set1 protein levels (Fig. 2B). When WT, Set1-S228A, and Set1-S228E

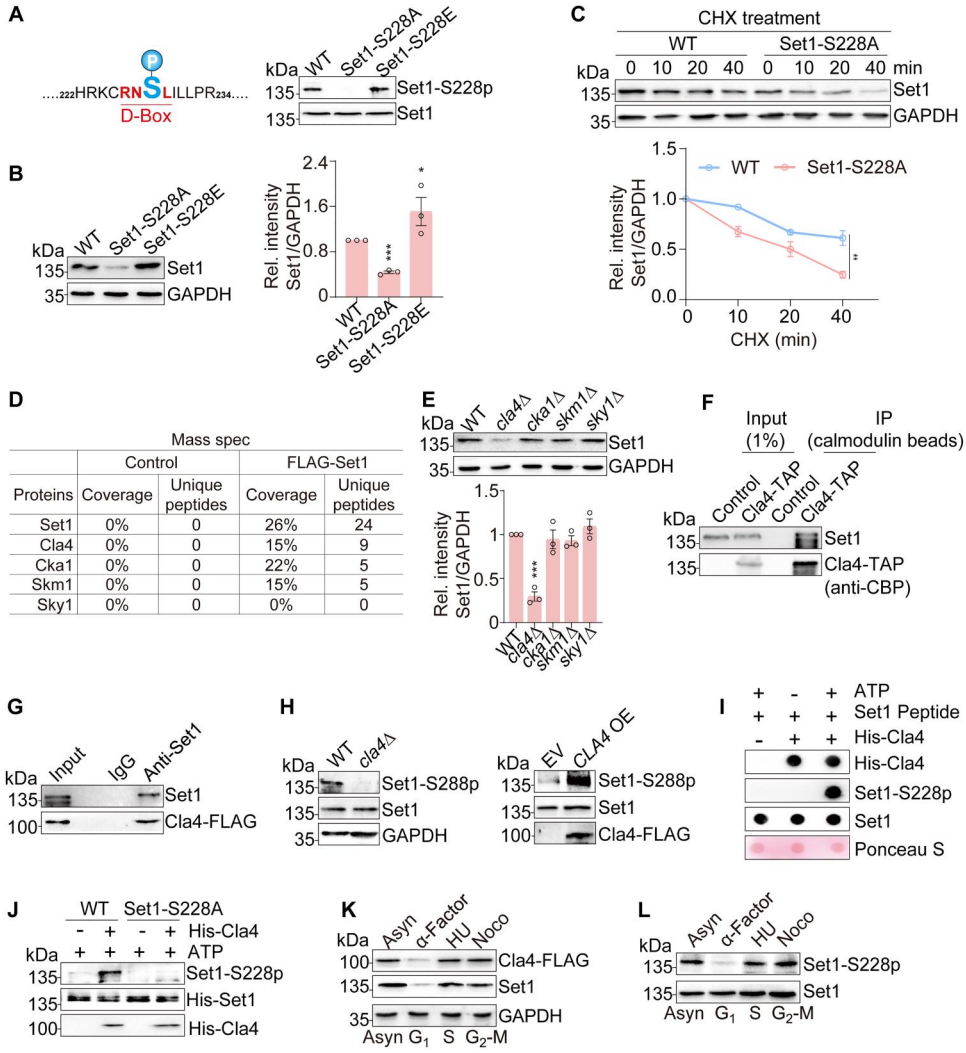

Fig. 2. Cla4 phosphorylates Set1-S228 to stabilize Set1. (**A**) Set1 was phosphorylated at S228 inside cells. Left panel: Diagram showing the predicted Set1-S228 phosphorylation site within the D-box. Right panel: Immunoblot analysis of Set1-S228 phosphorylation in WT, Set1-S228A, and Set1-S228E mutants with anti–Set1-S228p antibody. (**B**) Immunoblot analysis of Set1 protein levels in WT, Set1-S228A, and Set1-S228E mutants. (**C**) Immunoblot analysis of Set1 stability in WT and Set1-S228A mutant. WT and Set1-S228A mutant were treated with cycloheximide (CHX) (0.1 μg/ml) for 0 to 40 min. (**D**) Liquid chromatography–mass spectrometry analysis of proteins copurified with untagged FLAG-Set1. The identified unique peptides and sequence coverage were listed. (**E**) Immunoblot analysis of Set1 in WT, *cla4*Δ, *cka1*Δ, *skm1*Δ, and *sky1*Δ mutants. (**F** and **G**) Set1 interacted with Cla4 as determined by Co-IP assay (F) and reciprocal IP (G). Cells expressing untagged endogenous Cla4 were used as a negative control in (F). (**H**) Analysis of the effect of Cla4 on Set1-S228 phosphorylation. (**I**) In vitro kinase assay showing the purified recombinant His-Cla4 phosphorylated Set1 peptide. (**J**) Set1 was phosphorylated at S228 by the purified recombinant His-Cla4 in vitro. (**K** and **L**) Immunoblot analysis of Cla4, Set1, and Set1-S228p in cells that were arrested by α-factor, HU, or Noco of 3 hours. For (B), (C), and (E), data represent the mean ± SE of three biological independent experiments. **P* < 0.05, ***P* < 0.01, ****P* < 0.001.

mutants were treated with CHX, mutation of Set1-S228A shortened the half-life of Set1 and mutation of Set1-S228E prolonged the half-life of Set1 when compared with their WT counterpart (Fig. 2C and fig. S2D).

To characterize the potential protein kinase(s) that phosphorylates Set1-S228, we immunoprecipitated Set1 from cells and then subjected it to mass spectrometry analysis. The protein kinases Cla4, Cka1, and Skm1 were found to copurify with Set1 (Fig. 2D). We then examined Set1 protein levels in *cla4*Δ, *cka1*Δ, and *skm1*Δ mutants by immunoblots. The intracellular Set1 was significantly reduced in *cla4*Δ but not *cka1*Δ and *skm1*Δ mutants (Fig. 2E). Moreover, Set1-S228 conforms the consensus motif (RXS/T) for Cla4, which is the PAK and shows a strong selectivity for arginine residues two amino acid residues upstream of the phosphorylation site (*26*). The molecular docking showed that the sequence $_{226}$RNSL$_{229}$ of Set1 located in close proximity to Pak4, Cla4 homolog in mammals (fig. S2E). In addition, the Co-IP and reciprocal IP confirmed that the endogenous Cla4 interacted with Set1 (Fig. 2, F and G). Loss of Cla4 reduced the intracellular Set1-S228 phosphorylation, and overexpression of Cla4 increased Set1-S228 phosphorylation (Fig. 2H), indicating that Cla4 is the primary kinase to phosphorylate Set1-S228. To confirm that Cla4 can directly phosphorylate Set1-S228, we expressed and purified the recombinant Cla4 from *Escherichia coli* and performed the in vitro

kinase assay. Our results showed that the purified recombinant Cla4 can phosphorylate Set1 peptide (CRNS228LILLP) (Fig. 2I). The purified recombinant Cla4 can also phosphorylate the purified recombinant WT Set1 but not Set1-S228A mutant (Fig. 2J).

To determine whether Cla4 maintains Set1 protein levels by phosphorylating Set1-S228, we examined Set1 protein levels in WT, Set1-S228A, *cla4*Δ, and *cla4*Δ Set1-S228A mutants (fig. S3A). Loss of Set1-S228 phosphorylation reduced Set1 protein levels in Set1-S228A and *cla4*Δ mutants (fig. S3A). Deletion of *CLA4* did not further reduce Set1 protein level in Set1-S228A mutant (fig. S3A). Mutation of Set-S228E partly restored the Set1 protein levels in *cla4*Δ mutant (fig. S3B), suggesting that Cla4 phosphorylates Set1-S228 to enhance its stability.

As Set1 protein levels fluctuate throughout the cell cycle, we next examined the expression of Cla4 in the cell cycle. Cla4 protein levels were reduced in G_1 phase (Fig. 2K), which is similar to the trend of Set1 protein levels. Accordingly, Set1-S228 phosphorylation was also reduced in G_1 phase (Fig. 2L). To exclude the possibility that Cdh1 regulates Set1 protein levels indirectly by controlling Cla4 protein levels, we examined Cla4 expression in WT and *cdh1*Δ mutant and no significant difference was observed (fig. S3C). Overall, these data indicate that Cla4 phosphorylates Set1-S228 to maintain Set1 protein levels.

Cla4-catalyzed Set1-S228 phosphorylation prevents the APC/C^{Cdh1} complex–mediated Set1 degradation

Some posttranslational modifications regulate protein stability by affecting the interaction between the degradation machinery and target proteins (*27*). As Set1-S228 phosphorylation occurred within the context of D-box, we next examined whether Cla4-catalyzed Set1-S228 phosphorylation interferes with the interaction between Cdh1 and Set1. We purified WT FLAG-Set1 and FLAG-Set1-S228A from yeast cells, immobilized them on anti-FLAG beads, and then incubated them with the purified recombinant Cdh1. Cdh1 preferentially interacted with Set1-S228A when compared with WT Set1 (Fig. 3A, lane 6 versus lane 5). The mild interaction between WT FLAG-Set1 and Cdh1 could be due to incomplete phosphorylation of Set1 inside cells, or other Set1 domains may contribute to its interaction with Cdh1. We also performed the isothermal titration calorimetry (ITC) assay with the purified recombinant Cdh1 and Set1 peptides (CRNSLILLP) that contain either unphosphorylated S228 (Set1-S228) or phosphorylated S228 (Set1-S228p). Cdh1 showed higher binding affinity toward Set1-S228 peptide than Set1-S228p peptide (Fig. 3B). To directly determine the effect of Cla4-catalyzed Set1-S228 phosphorylation on the interaction between Set1 and Cdh1, we immobilized WT FLAG-Set1 on anti-FLAG beads and then incubated it with the purified recombinant Cla4 to phosphorylate Set1-S228. After 2-hour reaction, Cla4 was washed away and the purified recombinant Cdh1 was then added. As a control, FLAG-Set1-S228A was used in the parallel experiments. Cla4-catalyzed Set1-S228 phosphorylation markedly reduced the interaction between Set1 and Cdh1 (Fig. 3C, lane 1 versus lane 2). As a control, Set1-S228A showed higher binding to Cdh1 irrespective of Cla4 treatment (Fig. 3C, lane 3 versus lane 4).

To confirm whether Cla4-catalyzed Set1-S228 phosphorylation prevents APC/C^{Cdh1} complex–mediated Set1 polyubiquitination and proteolysis, we deleted *CDH1* in *cla4*Δ mutant. Loss of Cdh1 rescued the reduced Set1 in *cla4*Δ mutant (Fig. 3D). Meanwhile, loss of Cdh1 rescued the reduced Set1 in Set1-S228A mutant but had no marked effect on Set1 in Set1-S228E mutant (Fig. 3E). Moreover, the ubiquitination level of Set1 was significantly increased in Set1-S228A mutant but reduced in Set1-S228E mutant (Fig. 3F). We further performed in vitro ubiquitination assay with Set1 prephosphorylated by Cla4. Compared with unphosphorylated Set1, Cla4-catalyzed Set1 phosphorylation directly inhibited Cdh1-mediated Set1 polyubiquitination (Fig. 3G). These results demonstrate that Cla4-catalyzed Set1-S228 phosphorylation antagonizes APC/C^{Cdh1} complex–mediated polyubiquitination and subsequent degradation of Set1.

The PAF complex promotes Set1-S228 phosphorylation and enhances the stability of transcription-associated Set1

Set1 protein levels are linked to gene transcription and H3K4 methylation levels through a feedback regulatory mechanism (*17*). The recruitment of Set1 to chromatin is mediated by its association with the RNA Pol II elongation complex and depends on the presence of PAF complex and phosphorylation of the Rpb1 CTD (*13*, *14*). Although the N-terminal 780 amino acids of Set1 have been reported to destabilize Set1 in response to transcription inhibition, loss of the PAF complex, and mutation of H3K4 (*17*), little is known about the underlying mechanism. We wondered whether Cla4-catalyzed Set1-S228 phosphorylation is involved in transcription-associated stabilization of Set1. Consistent with reported results (*17*), deletion of the PAF complex subunits, *PAF1* and *RTF1*, reduced the global level of Set1 (Fig. 4A). Accordingly, treatment with 6-azauracil (6AU) to inhibit transcription elongation also reduced Set1 protein levels and this reduction was not caused by *SET1* transcriptional repression by 6AU (fig. S4, A and B). Moreover, knockdown of Kin28 that phosphorylates RNA Pol II CTD repeats at Ser^5 also significantly reduced Set1 protein levels but not its transcription levels (fig. S4, C and D). To determine whether the reduced Set1 in *paf1*Δ mutant was associated with the cell cycle, we synchronized WT and *paf1*Δ mutant at G_1 phase with α-factor, S phase with HU, and G_2-M phase with Noco, respectively. Loss of Paf1 reduced Set1 in all synchronized cells (fig. S4E), suggesting that the PAF complex regulates Set1 expression irrespective of the cell cycle.

We then determined whether Cla4-catalyzed Set1-S228 phosphorylation is involved in stabilization of Set1 by the above factors. Knockdown of Kin28 reduced the intracellular Set1-S228 phosphorylation (fig. S4F). Set1-S228 phosphorylation was also substantially reduced in the *paf1*Δ and *rtf1*Δ mutants (Fig. 4B). By analyzing the mass spectrometry data for FLAG-Set1 and Cla4-FLAG, we identified the presence of peptides corresponding to the PAF complex subunits, including Paf1, Cdc73, Rtf1, Leo1, and Ctr9 (Fig. 4C). The interaction among Set1, Cla4, and the PAF complex was confirmed by Co-IP and reciprocal IP (Fig. 4D). On the basis of these observations, we hypothesized that the PAF complex may enhance the interaction between Cla4 and Set1 to promote Set1-S228 phosphorylation. To test this, we examined the effect of PAF complex on the interaction between Cla4 and Set1 by Co-IP. Loss of Paf1 reduced the interaction between Cla4 and Set1 (Fig. 4E, lane 3 versus lane 4). We also performed Co-IP with purified PAF complex (Ctr9-TAP), Set1, and Cla4. The in vitro Co-IP showed that the PAF complex directly enhanced the interaction between Cla4 and Set1 (Fig. 4F). Moreover, we performed the in vitro kinase assay with the purified recombinant Cla4 and Set1 in the presence or absence of purified PAF complex.

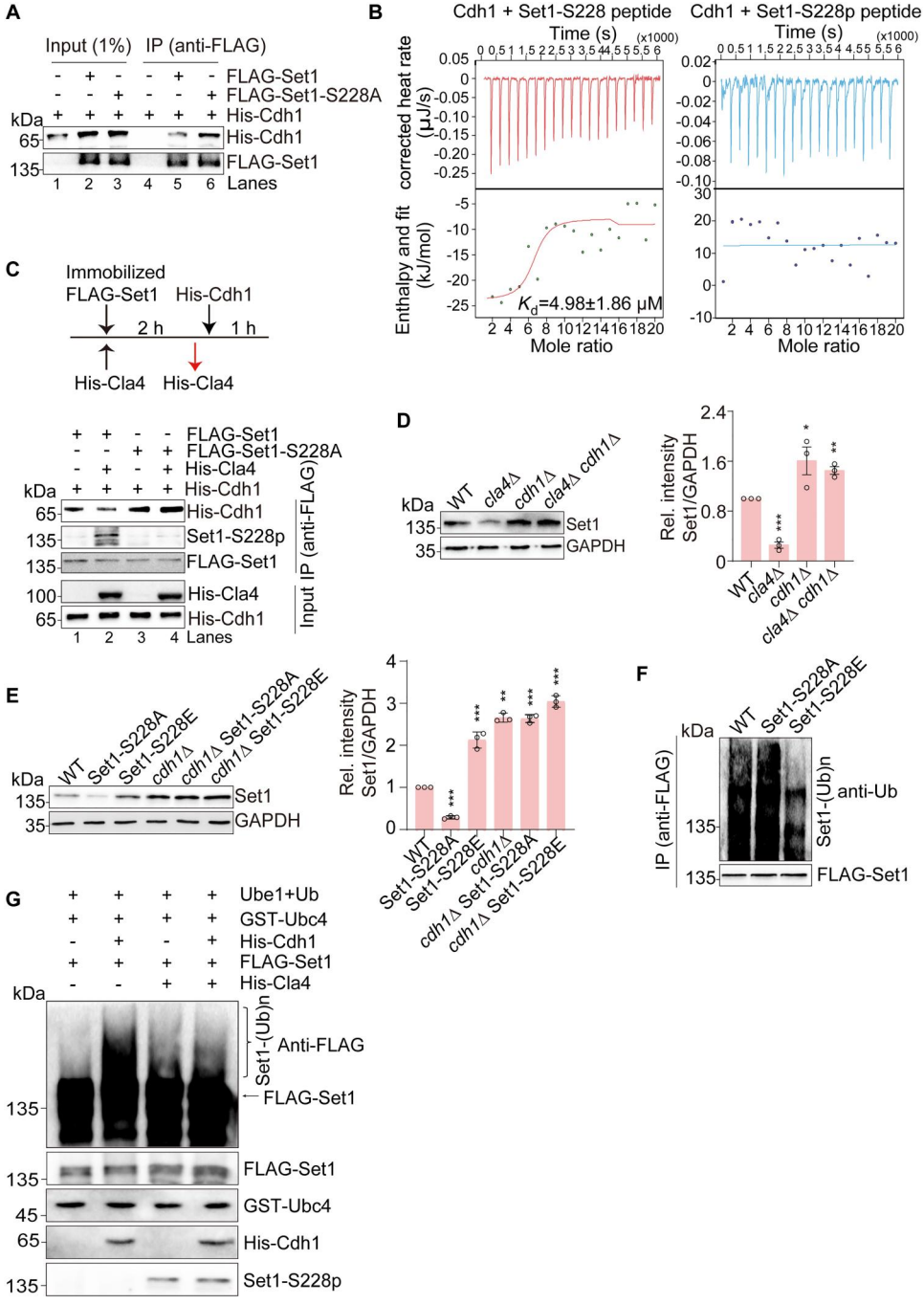

Fig. 3. Set1-S228 phosphorylation prevents Cdh1-mediated Set1 degradation. (**A**) Cdh1 preferentially interacted with Set1-S228A mutant as determined by Co-IP. FLAG-Set1 and FLAG-Set1-S228A were immunoprecipitated with anti-FLAG agarose and then incubated with purified recombinant His-Cdh1. (**B**) Isothermal titration calorimetry (ITC) assay showing that Cdh1 had a higher binding affinity toward Set1-S228 peptide than Set1-S228p peptide. (**C**) Cla4-catalyzed Set1-S228 phosphorylation reduced the interaction between Set1 and Cdh1. FLAG-Set1 and FLAG-Set1-S228A were immobilized with anti-FLAG agarose. The purified recombinant His-Cla4 was added to phosphorylate Set1 for 2 hours. After His-Cla4 was washed away, the immobilized Set1 was incubated with the purified recombinant His-Cdh1 for 1 hour. (**D**) Immunoblot analysis of Set1 in WT, *cla4*Δ, *cdh1*Δ, and *cla4*Δ *cdh1*Δ mutants. (**E**) Immunoblot analysis of Set1 in WT, Set1-S228A, Set1-S228E, *cdh1*Δ, *cdh1*Δ Set1-S228A, and *cdh1*Δ Set1-S228E mutants. (**F**) Analysis of the ubiquitination of Set1 in WT, Set1-S228A, and Set1-S228E mutants. (**G**) In vitro ubiquitination assay showing that Cla4-catalyzed Set1-S228 phosphorylation inhibited Cdh1-mediated Set1 polyubiquitination. The immobilized FLAG-Set1 was first phosphorylated by His-Cla4. After His-Cla4 was washed away, phosphorylated Set1 was then incubated with Cdh1, Ube1, Ubc4, adenosine triphosphate (ATP), and free ubiquitin. The unphosphorylated Set1 was used as a control. For (D) and (E), data represent the mean ± SE of three biological independent experiments. **P* < 0.05, ***P* < 0.01, ****P* < 0.001.

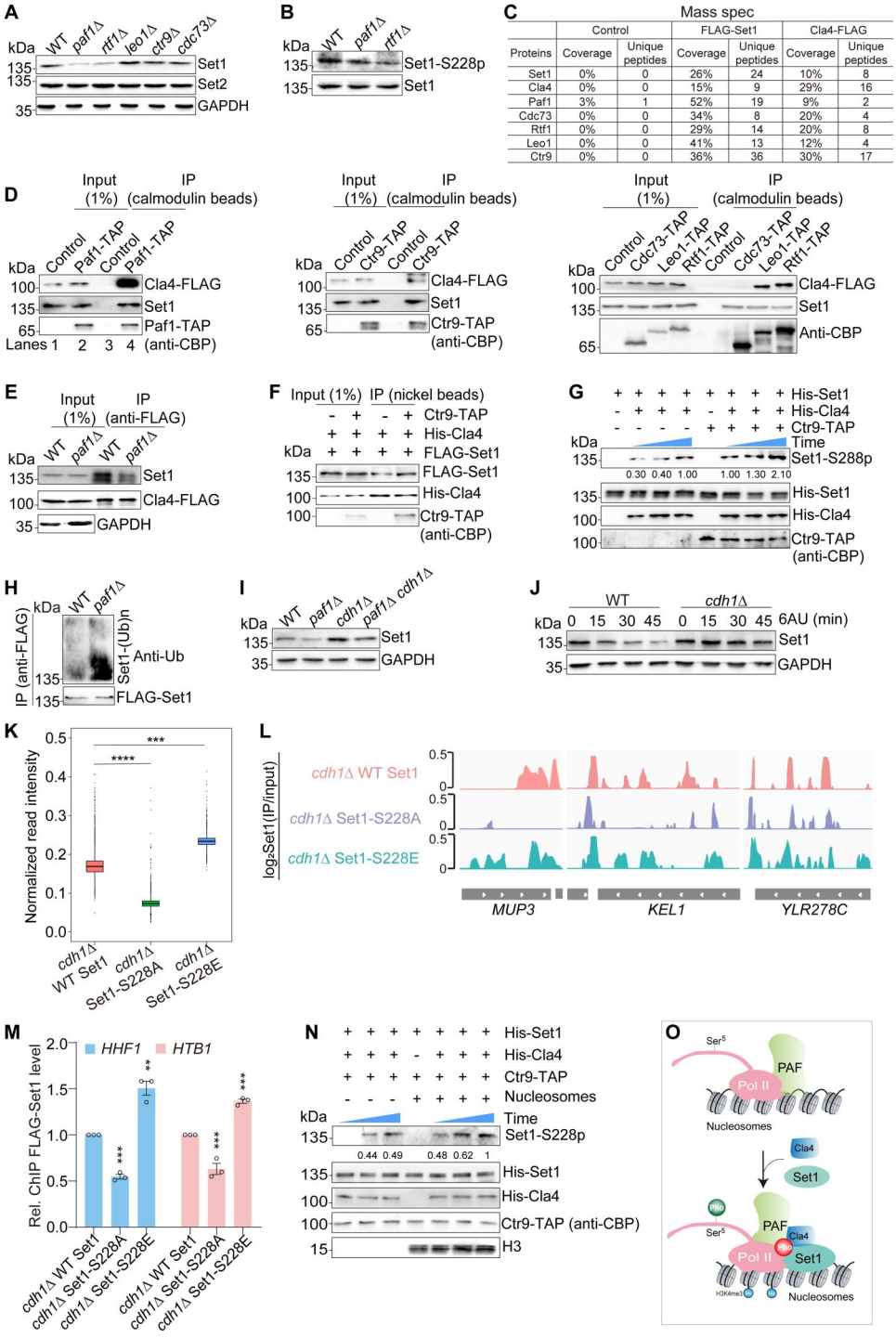

Fig. 4. The PAF complex facilitates Cla4 to phosphorylate Set1-S228 and stabilize Set1. (**A**) Immunoblot analysis of Set1 in WT and PAF complex mutants. (**B**) Immunoblot analysis of Set1-S228 phosphorylation in WT, *paf1*Δ, and *rtf1*Δ mutants. (**C**) IP–mass spectrometry analysis of proteins copurified with Set1 and Cla4. (**D**) Cla4 interacted with PAF complex as determined by Co-IP assay. (**E**) Loss of Paf1 reduced Set1-Cla4 interaction. (**F**) In vitro Co-IP assay showing that PAF complex enhances Set1-Cla4 interaction. The purified FLAG-Set1 was incubated with His-Cla4 with or without purified PAF complex (Ctr9-TAP). (**G**) PAF complex facilitates Cla4 to phosphorylate Set1-S228. The purified His-Set1 was incubated with His-Cla4 with or without purified PAF complex (Ctr9-TAP). (**H**) Immunoblot analysis of Set1 ubiquitination in WT and *paf1*Δ mutant. (**I**) Immunoblot analysis of Set1 in WT, *paf1*Δ, *cdh1*Δ, and *paf1*Δ *cdh1*Δ mutants. (**J**) Immunoblot analysis of Set1 in WT and *cdh1*Δ mutant when treated with 6AU for 0 to 45 min. (**K**) Box plots showing the normalized read intensity of Set1 occupancy at chromatin in *cdh1*Δ WT Set1, *cdh1*Δ Set1-S228A, and *cdh1*Δ Set1-S228E mutants. Center-lines denote medians, box limits denote 25th and 75th percentiles, and whiskers denote maximum and minimum values. Two-sided Wilcoxon test in R (package ggpval) was used for statistical analysis. (**L**) ChIP-seq tracks of Set1 occupancy at indicated genes in *cdh1*Δ WT Set1, *cdh1*Δ Set1-S228A, and *cdh1*Δ Set1-S228E mutants. (**M**) ChIP-qPCR analysis of Set1 occupancy at indicated genes in *cdh1*Δ WT Set1, *cdh1*Δ Set1-S228A, and *cdh1*Δ Set1-S228E mutants. (**N**) Nucleosomes facilitates Cla4 to phosphorylate Set1-S228. The purified His-Set1 was incubated with His-Cla4 and PAF complex with or without nucleosomes. (**O**) Diagram showing that Cla4-mediated Set1-S228 phosphorylation was facilitated by PAF complex and RNA Pol II. For (M), data represent the mean ± SE of three biological independent experiments. $^{*}P < 0.05$, $^{**}P < 0.01$, $^{***}P < 0.001$.

Addition of the PAF complex enhanced the ability of Cla4 to phosphorylate Set1-S228 (Fig. 4G). These results suggest that the PAF complex can enhance the interaction between Cla4 and Set1 to promote Set1-S228 phosphorylation.

We then examined whether the PAF complex maintains Set1 protein stability by protecting it from APC/C^{Cdh1}-mediated polyubiquitination and subsequent proteolysis. Loss of Paf1 increased the polyubiquitination of Set1, leading to its degradation (Fig. 4, H and I). Deletion of *CDH1* rescued the reduced Set1 in *paf1*Δ mutant (Fig. 4I and fig. S4G). Loss of Cdh1 also restored the reduced Set1 by 6AU treatment (Fig. 4J).

The Set1 N-terminal region has been reported to interact with RNA Pol II and facilitate the recruitment of COMPASS complex to chromatin (*28*). We thus examined the effect of Set1-S228 phosphorylation on the binding of Set1 to chromatin. To exclude the possibility that the difference may come from changes of Set1

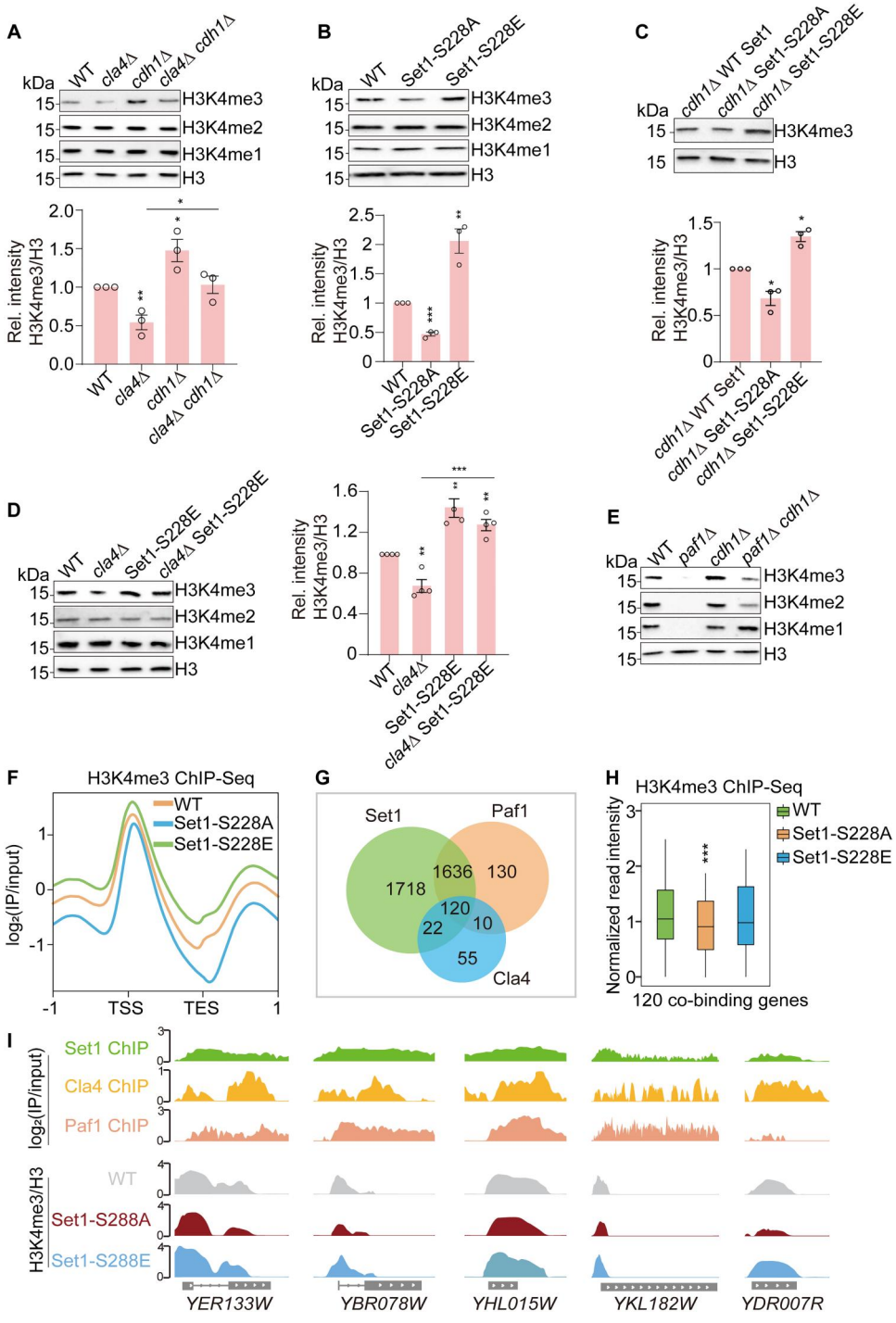

Fig. 5. Cla4-catalyzed Set1-S228 phosphorylation promotes Set1-catalyzed H3K4me3. (**A**) Immunoblot analysis of H3K4me1, H3K4me2, and H3K4me3 in WT, *cla4*Δ, *cdh1*Δ, and *cla4*Δ *cdh1*Δ mutants. (**B**) Immunoblot analysis of H3K4me1, H3K4me2, and H3K4me3 in WT, Set1-S228A, and Set1-S228E mutants. (**C**) Immunoblot analysis of H3K4me3 in *cdh1*Δ WT Set1, *cdh1*Δ Set1-S228A, and *cdh1*Δ Set1-S228E mutants. (**D**) Immunoblot analysis of H3K4me1, H3K4me2, and H3K4me3 in WT, *cla4*Δ, Set1-S228E, and *cla4*Δ Set1-S228E mutants. (**E**) Immunoblot analysis of H3K4me1, H3K4me2, and H3K4me3 in WT, *paf1*Δ, *cdh1*Δ, and *paf1*Δ *cdh1*Δ mutants. (**F**) Average metagene profiles of H3K4me3 in WT, Set1-S228A, and Set1-S228E mutants. (**G**) Venn diagram of genes that overlap among the Set1-peak, Paf1-peak, and Cla4-peak gene sets as determined by ChIP-seq. The numbers of binding sites are represented. (**H**) Box plots showing the normalized read intensity of H3K4me3 in WT, Set1-S228A, and Set1-S228E mutants. Centerlines denote medians, box limits denote 25th and 75th percentiles, and whiskers denote maximum and minimum values. Two-sided Wilcoxon test in R (package ggpval) was used for statistical analysis. (**I**) ChIP-seq tracks of Set1, Cla4, and Paf1 occupancy in WT cells as well as H3K4me3/H3 enrichment in WT, Set1-S228A, and Set1-S228E mutants at indicated genes. For (A) to (C), data represent the mean ± SE of three biological independent experiments. For (D), data represent the mean ± SE of four biological independent experiments. **P* < 0.05, ***P* < 0.01, ****P* < 0.001.

protein levels, we deleted *CDH1* in WT, Set1-S228A, and Set1-S228E mutants and then immunoprecipitated Set1. Loss of Set1-S228 phosphorylation in Set1-S228A mutant led to less nucleosomes associated with Set1 (fig. S4H, lane 4 versus lane 5), while more nucleosomes were associated with Set1-S228E mutant (fig. S4H, lane 4 versus lane 6). We also performed ChIP-seq (chromatin immunoprecipitation with high-throughput sequencing) for Set1 in *cdh1*Δ WT Set1, *cdh1*Δ Set1-S228A, and *cdh1*Δ Set1-S228E mutants. Although Set1 degradation was blocked in these mutants, the binding of Set1-S228A to chromatin was reduced and the binding of Set1-S228E to chromatin was increased when compared with WT Set1 (Fig. 4, K and L), which was also confirmed by ChIP-qPCR (quantitative polymerase chain reaction) (Fig. 4M). To determine how Set1-S228 phosphorylation promotes Set1 binding to chromatin, we examined the interaction between Set1 and RNA Pol II subunit Rpb3. Our data showed that Set1-S228A had reduced interaction with Rpb3, while Set1-S228E had increased interaction with Rpb3 (fig. S4I). Set1-S228A also showed reduced interaction with COMPASS subunit Spp1 (fig. S4J), which has been reported to promote Set1 binding to chromatin (*29*).

Next, to examine whether the chromatin association of Set1 enhances the Set1-S228 phosphorylation, we performed the in vitro kinase assay with purified Set1, PAF complex, and Cla4 in the presence or absence of nucleosomes. Our data showed that addition of nucleosomes directly enhanced Set1-S228 phosphorylation (Fig. 4N). As for how chromatin association facilitates Set1-S228 phosphorylation, it is possible that binding to chromatin may lead to conformational change of Set1, which then enhances its phosphorylation by Cla4.

As the PAF complex promotes Set1 binding to chromatin (*13*, *14*), we examined the binding of Set1 at chromatin in WT, *paf1*Δ, *cdh1*Δ, and *paf1*Δ *cdh1*Δ mutants. The binding of Set1 at chromatin was reduced in *paf1*Δ mutant, and loss of Cdh1 partly restored the binding of Set1 at chromatin (fig. S4K). As nucleosomes can promote Set1-S228 phosphorylation (Fig. 4N), it is highly likely that the PAF complex could also enhance Set1 stability by recruiting Set1 binding to chromatin. Together, these data suggest that the PAF complex not only facilitates the interaction between Cla4 and Set1 but also promotes Set1 binding to chromatin, which could together enhance Cla4 to phosphorylate Set1-S228 and stabilize Set1 during gene transcription (Fig. 4O).

Cla4-catalyzed Set1-S228 phosphorylation promotes Set1-catalyzed H3K4me3

The above results demonstrate that Cla4 phosphorylates Set1-S228 to stabilize Set1 by inhibiting its recognition and degradation mediated by the APC/C^{Cdh1} complex. This regulation occurred within the cell cycle and during gene transcription. We next examined the effect of Cla4-catalyzed Set1-S228 phosphorylation and the APC/C^{Cdh1} complex on Set1-catalyzed H3K4 methylation. Consistent with Set1 changes, the intracellular levels of H3K4 methylation, especially H3K4me3, were reduced in *cla4*Δ mutant and increased in *cdh1*Δ mutant (fig. S5, A and B). This marked change of H3K4me3 suggests that H3K4me3 is more sensitive to Set1 protein level changes when compared with H3K4me2 and H3K4me1. Several mutations, including Set1 point mutation (K1007/8A) and H3K14A, have been reported to reduce Set1 protein levels and impair H3K4me3 with mild effect on H3K4me1 and H3K4me2 (*16*, *17*). Loss of Cdh1 partly rescued the reduced H3K4me3 in *cla4*Δ mutant (Fig. 5A). The levels of H3K4me3 were reduced in Set1-S228A mutant but increased in Set1-S228E mutant (Fig. 5B). Loss of Cdh1 partly restored the reduced H3K4me3 in Set1-S228A mutant (Fig. 5C and fig. S5C). Compared with *cdh1*Δ mutant, H3K4me3 was still reduced in *cdh1*Δ Set1-S228A mutant (Fig. 5C), which is consistent with reduced Set1 binding at chromatin in *cdh1*Δ Set1-S228A mutant (Fig. 4, K to M), suggesting that Set1-S228 phosphorylation contributes to H3K4me3 not only by stabilizing Set1 but also by facilitating Set1 binding to chromatin. Mutation of Set1-S228E rescued the reduced H3K4me3 in *cla4*Δ mutant (Fig. 5D), suggesting that Cla4 phosphorylates Set1-S228 to enhance Set1-catalyzed H3K4me3. Moreover, we examined H3K4 methylation in WT, *paf1*Δ, *cdh1*Δ, and *paf1*Δ *cdh1*Δ mutants. H3K4 mono-methylation (H3K4me1) was reduced in *paf1*Δ mutant but was restored in *paf1*Δ *cdh1*Δ mutant (Fig. 5E). H3K4 di-methylation (H3K4me2) and H3K4me3 were partially rescued in *paf1*Δ *cdh1*Δ mutant (Fig. 5E). As the PAF complex promotes Set1 binding to chromatin and loss of Cdh1 partly restored the binding of Set1 at chromatin (fig. S4K), the partial rescue of H3K4me3 in *paf1*Δ *cdh1*Δ mutant suggested that the PAF complex contributes to H3K4 methylation not only by preventing Set1 degradation but also by enhancing the chromatin association of Set1.

We then examined Cla4-catalyzed Set1-S228 phosphorylation on genome-wide occupancy of H3K4me3 by ChIP-seq. The enrichment of H3K4me3 was reduced in Set1-S228A mutant but was increased in Set1-S228E mutant (Fig. 5F). To examine whether Cla4, Set1, and the PAF complex colocalized at chromatin, we performed ChIP-seq for Cla4 and compared it with the ChIP-seq data of Set1 and Paf1. ChIP-seq analysis revealed that 68% and 62.5% of Cla4-bound genes were co-occupied by Set1 and Paf1, respectively (fig. S5D). Set1, Paf1, and Cla4 colocalized at a total of 120 genes (Fig. 5G). KEGG (Kyoto Encyclopedia of Genes and Genomes) analysis revealed that these 120 genes were enriched in ribosome, biosynthesis of antibiotics, glycolysis/gluconeogenesis, etc. (fig. S5E). The enrichment of H3K4me3 at these 120 genes was also significantly reduced in Set1-S228A mutant (Fig. 5, H and I), suggesting that the PAF complex may enhance Set1-S228 phosphorylation and promote Set1-catalyzed H3K4me3 at these genes.

Cla4-catalyzed Set1-S228 phosphorylation regulates gene transcription, telomere silencing, and longevity

Among 120 genes co-occupied by Set1, Cla4, and Paf1, 8 core histone genes were enriched with Set1, Cla4, and Paf1 (Fig. 6A). Moreover, Set1-catalyzed H3K4me3 has been reported to promote histone gene expression (*18*). We thus examined the effect of Cla4-catalyzed Set1-S228 phosphorylation on histone gene expression. The transcription of core histones was significantly reduced in *cla4*Δ mutant but increased in *cdh1*Δ mutant (fig. S6A). Both the mRNA and protein levels of core histones were significantly reduced in Set1-S228A mutant but significantly increased in Set1-S228E mutant (Fig. 6, B and C). In addition, we synchronized WT, Set1-S228A, and Set1-S228E mutants and then released into different cell cycle phases. Mutation of Set1-S228A significantly reduced the transcription of core histone genes during S phase, while Set1-S228E significantly increased the transcription of histone genes during S phase (fig. S6B), which are consistent with our reports that Set1 regulates the transcription of core histones primarily at S phase (*18*). We then examined the protein

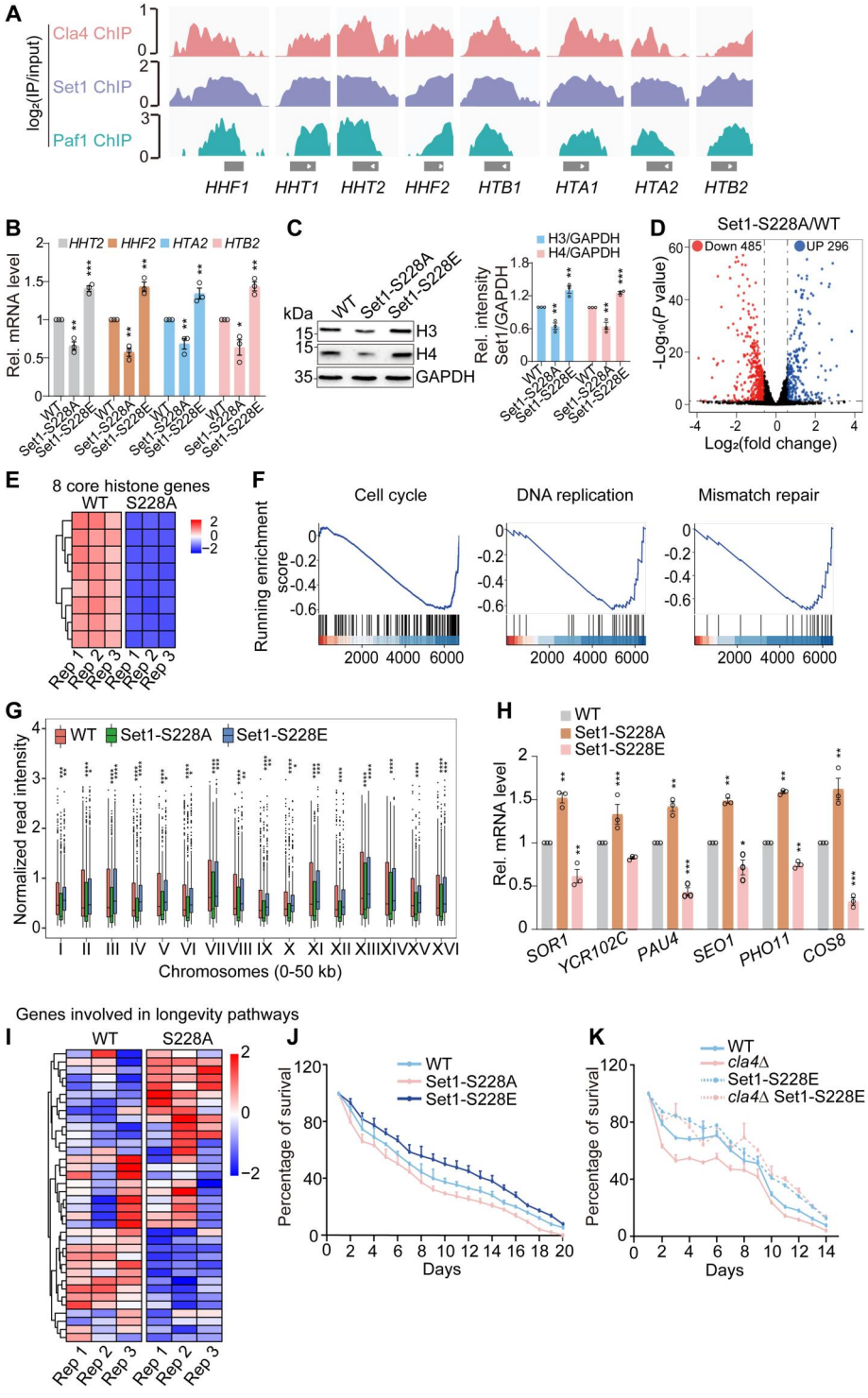

Fig. 6. Cla4 and Cdh1 regulate gene transcription and chronological life span by affecting Set1 stability. (**A**) ChIP-seq tracks of Set1, Cla4, and Paf1 occupancy at eight core histone genes. (**B**) RT-qPCR analysis of core histone gene transcription in WT, Set1-S228A, and Set1-S228E mutants. *HHT2* encodes histone H3; *HHF2* encodes histone H4; *HTA2* encodes histone H2A; *HTB2* encodes histone H2B. (**C**) Immunoblot analysis of core histones in WT, Set1-S228A, and Set1-S228E mutants. (**D**) Volcano plots for genes differentially expressed in WT and Set1-S228A mutant. Differential expression levels of aligned sequences were calculated using significant thresholds set at $\log_2(FC) \leq -0.75$, $\log_2(FC) \geq 0.75$, $P < 0.05$. Red color designates significantly down-regulated genes, and blue color designates significantly up-regulated genes. (**E**) Heatmap showing the transcription of eight core histone genes in WT and Set1-S228A mutant. (**F**) GSEA analysis of genes involved in cell cycle, DNA replication, and mismatch repair in WT and Set1-S228A mutant. (**G**) Box plots showing the normalized read intensity of H3K4me3 at subtelomeric regions on 16 chromosomes in WT, Set1-S228A, and Set1-S228E mutants. The subtelomeric regions refer to 0 to 50 kb from the nearest left or right telomeres. (**H**) RT-qPCR analysis of the transcription of telomere-proximal genes in WT, Set1-S228A, and Set1-S228E mutants. (**I**) Heatmap showing the transcription of the longevity pathway genes in WT and Set1-S228A mutant. (**J**) Chronological life-span analysis of WT, Set1-S228A, and Set1-S228E mutants. (**K**) Chronological life-span analysis of WT, *cla4*Δ, Set1-S228E, and Set1-S228E *cla4*Δ mutants. For (B), (C), (H), (J), and (K), data represent the mean ± SE of three biological independent experiments. *$P < 0.05$, **$P < 0.01$, ***$P < 0.001$.

levels of core histones in these mutants. Core histones were reduced in Set1-S228A mutant, and loss of Cdh1 partly rescued the reduced core histones in Set1-S228A mutant (fig. S6C). Core histones were reduced in *cla4*Δ mutant, and mutation of Set1-S228E partly rescued the reduced core histones in *cla4*Δ mutant (fig. S6C). Likewise, loss of Cdh1 partly restored the reduced core histones in *cla4*Δ and *paf1*Δ mutants (fig. S6, D and E).

H3K4me3 is deposited by Set1 at the promoter of active genes, i.e., *GAL1* after induction by galactose and H3K4me3 can persist after transcriptional inactivation for considerable time, constituting a transcriptional memory for recent transcriptional activity (*13*). It has been reported that ablation of H3K4me3 increases the reactivation of genes, i.e., *GAL1* (*30*). As Cla4-catalyzed Set1-S228 phosphorylation regulates Set1 protein levels as well as H3K4me3, we

then examined the transcription kinetics of *GAL1* upon galactose induction and re-induction. Briefly, long-term glucose-cultured (LT-Glc) yeast cells were shifted into galactose culture for 2.5 hours (initial induction). The cells were then shifted back to glucose-containing medium for an additional 1 hour to repress *GAL1*. Finally, the short-term repressed cells were re-induced by galactose (re-induction) (fig. S6F). During the initial induction, the transcription of *GAL1* was increased in *cla4*Δ and Set1-S228A mutants but reduced in *cdh1*Δ and Set1-S228E mutants (fig. S6F). Compared with initial induction, the re-induction of *GAL1* rapidly occurred in WT and this re-induction was more rapid in *cla4*Δ and Set1-S228A mutants (fig. S6F). This re-induction was slower in *cdh1*Δ and Set1-S228E mutants when compared with WT cells (fig. S6F). Mutation of Set1-S228E partly rescued the increased *GAL1* expression kinetics in *cla4*Δ mutant (fig. S6F). Loss of Cdh1 also partly rescued the increased *GAL1* expression kinetics in *cla4*Δ and Set1-S228A mutants (fig. S6F).

To explore the effect of Cla4-catalyzed Set1-S228 phosphorylation on genome-wide gene transcription, we performed RNA-seq (RNA sequencing) for WT and Set1-S228A mutant. By analyzing the RNA-seq data for WT and Set1-S228A mutant, 485 genes were significantly down-regulated and 296 genes were significantly up-regulated in Set1-S228A mutant ($\log_2(FC) \leq -0.75$, $\log_2(FC) \geq 0.75$; $P < 0.05$) (Fig. 6D). All eight core histone genes were significantly reduced in Set1-S228A mutant (Fig. 6E), consistent with our reverse transcription qPCR (RT-qPCR) results (Fig. 6B). KEGG analysis revealed that these differentially regulated genes in Set1-S228A mutant were enriched in cell cycle, mitogen-activated protein kinase (MAPK) signaling pathway, meiosis, DNA replication, amino sugar and nucleotide sugar metabolism, mismatch repair, and homologous recombination (fig. S6G). GSEA (Gene Set Enrichment Analysis) analysis revealed that genes involved in cell cycle, DNA replication, and mismatch repair were significantly regulated in Set1-S228A mutant (Fig. 6F). In line with the above results, mutation of Set1-S228A also reduced normal cell cycle progression by causing an arrest at G_1/S (fig. S6H).

Set1-catalyzed H3K4me3 has been reported to regulate telomere silencing (*31*). Loss of Set1 disrupts telomere heterochromatin structure and increases the transcription of telomere-proximal genes (*31*). Mutation of Set1-S228A reduced H3K4me3 occupancy at subtelomere regions, while mutation of Set1-S228E increased H3K4me3 occupancy at subtelomere regions (Fig. 6G). To determine whether Cla4-catalyzed Set1-S228 phosphorylation regulates telomere silencing, we examined the transcription of telomere-proximal genes, including *SOR1*, *YCR102C*, *PAU4*, *SEO1*, *PHO11*, and *COS8*, which are located 9.1, 11.1, 14.9, 7.2, 3.3, and 6.4 kb to the telomere ends of chromosomes X-R, III-R, XII-R, I-L, I-R, and VIII-L, respectively. These genes were increased in Set1-S228A but reduced in Set1-S228E mutant (Fig. 6H), which is consistent with the changes of Set1 protein levels. Loss of Cdh1 restored the increased transcription of these telomere-proximal genes in Set1-S228A mutant (fig. S6I). In line with these observations, these telomere-proximal genes were significantly increased in *cla4*Δ mutant and mutation of Set1-S228E restored the increased transcription of telomere-proximal genes in *cla4*Δ mutant (fig. S6J). These data suggest that Cla4-catalyzed Set1-S228 phosphorylation is required to maintain normal telomere silencing.

The expression of core histones tightly controls the chronological life span (*18*). By analyzing the RNA-seq data, we also found that genes involved in the longevity pathway were differentially regulated in Set1-S228A mutant (Fig. 6I). We therefore examined the effect of Cla4-catalyzed Set1-S228 phosphorylation on the chronological life span. The chronological life span of Set1-S228A mutant was reduced and the chronological life span of Set1-S228E mutant was increased when compared with WT (Fig. 6J). Moreover, loss of Cla4 reduced the chronological life span and mutation of Set1-S228E extended the chronological life span of *cla4*Δ mutant (Fig. 6K).

Collectively, these results indicate that Cla4 phosphorylates Set1-S228 to maintain H3K4me3, which then regulates gene transcription, telomere silencing, and chronological life span.

Cla4 and APC/C^{Cdh1} regulate the stability of yeast proteins at the proteome level

Next, we wondered whether there are other yeast proteins whose stability is co-regulated by Cla4 and the APC/C^{Cdh1} complex in addition to Set1. We searched for proteins that can be regulated by Cla4 and the APC/C^{Cdh1} complex at the proteome level by combining bioinformatic tools and mass spectrometry. The APC/C^{Cdh1} complex recognizes the consensus sequence (RXXL) of the D-box, and Cla4 phosphorylates the RXS/T motif. If the stability of target proteins is co-regulated by the APC/C^{Cdh1} complex and Cla4, they need to contain the motif (RXS/TL) that can be recognized by the APC/C^{Cdh1} complex and degraded by the proteasome pathway. Meanwhile, the motif (RXS/TL) should also be phosphorylated by Cla4, which then protects proteins from APC/C^{Cdh1}-mediated degradation. We thus called the phosphorylated RXS/TL (RXpS/TL) motif as the protection box (P-box). Using bioinformatics analysis, we identified a total of 1224 proteins that contain the predicted RXS/TL motif (Fig. 7A). Among these 1224 proteins, 1050 proteins were found to interact with Cla4 as determined by mass spectrometry of Cla4-FLAG (Fig. 7A). Among these 1050 proteins, 141 proteins were found to be phosphorylated at the RXS/TL motif (RXpS/TL, P-box) as determined by mass spectrometry (Fig. 7A). KEGG analysis of these 141 P-box–containing proteins revealed that they were enriched in cell cycle, meiosis, glycerophospholipid metabolism, and autophagy pathways (Fig. 7B, fig. S7A, and table S1).

To examine whether the above 141 proteins were regulated by Cla4 and Cdh1, we randomly chose 7 proteins from these pathways and examined their expression in cells synchronized at G_1, S, and G_2-M phases. These proteins include two proteins (Gin4 and Smc3) from cell cycle, three proteins (Chd1, Sin3, and Sas4) from chromatin and telomere pathway, Sln1 from RNA-related pathway, and Atg9 from autophagy pathway. Similar to the changes of Set1 protein levels, their protein levels were specifically reduced in G_1 phase (Fig. 7C and fig. S7B), implying that their expression oscillates with the cell cycle.

Among these seven proteins, Gin4 contains two P-boxes ($_{500}$RMpSL$_{504}$ and $_{1094}$RSpTL$_{1097}$) and Smc3 contains one P-box ($_{428}$RTpSL$_{431}$). We then examined whether these two proteins are regulated by Cla4 and Cdh1. Loss of Cla4 significantly reduced the intracellular levels of both Gin4 and Smc3, and deletion of *CDH1* increased their protein levels (Fig. 7, D and E, and fig. S7, C and D). Loss of Cdh1 restored the reduced expression of Gin4 and Smc3 in *cla4*Δ mutant (Fig. 7, D and E). All these data suggest that Cla4 may phosphorylate these two proteins and

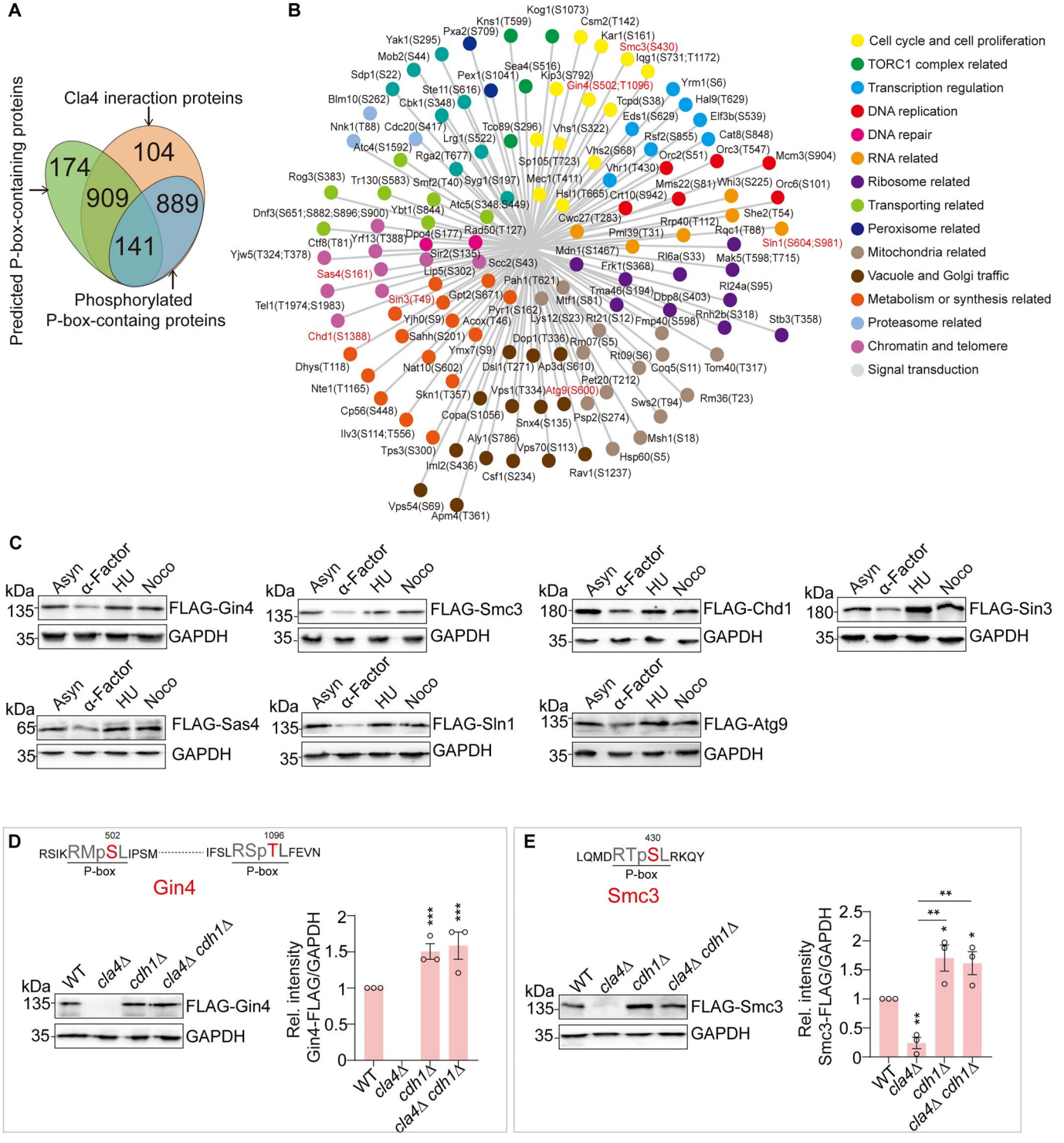

Fig. 7. Cla4 and Cdh1 co-regulate the stability of yeast proteins at the proteome level. (**A**) Venn diagram of proteins that were predicted to contain P-box, interact with Cla4, and phosphorylate at P-box. (**B**) Proteins containing phosphorylated P-box were categorized by gene ontology (GO) annotations. Proteins that were confirmed to be regulated by Cla4 and Cdh1 were labeled in red. (**C**) Immunoblot analysis of the expression of Gin4, Smc3, Chd1, Sin3, Sas4, Sln1, and Atg9 in cells that were arrested in G_1, S, and G_2-M using α-factor (10 μg/ml), 10 μM HU, and 8 μM Noco for 3 hours, respectively. (**D**) Immunoblot analysis of Gin4 in WT, *cla4*Δ, *cdh1*Δ, and *cla4*Δ *cdh1*Δ mutants. The two P-boxes within Gin4 were indicated with red color. (**E**) Immunoblot analysis of Smc3 protein levels in WT, *cla4*Δ, *cdh1*Δ, and *cla4*Δ *cdh1*Δ mutants. The P-box within Smc3 was indicated with red color. For (D) and (E), data represent the mean ± SE of three biological independent experiments. **P* < 0.05, ***P* < 0.01, ****P* < 0.001.

protect them from APC/C^{Cdh1}-mediated polyubiquitination and subsequent degradation.

DISCUSSION

Set1-catalyzed H3K4me3 has been reported to promote core histone gene expression and maintain normal chronological life span (*18*, *19*). The transcription of core histone genes is tightly regulated by the cell cycle (*18*, *20*). Here, we report that Set1 protein levels oscillate throughout the cell cycle and its stability is co-regulated by Cla4 and the APC/C^{Cdh1} complex. The N-terminal domain of Set1 contains a D-box, which enables Set1 to be ubiquitinated by the APC/C^{Cdh1} complex followed by degradation in the G_1 phase. Meanwhile, Cla4 phosphorylates Set1-S228 within the D-box, which antagonizes APC/C^{Cdh1}-mediated Set1 degradation and facilitates the chromatin association of Set1. During gene transcription, the PAF complex promotes Cla4 to phosphorylate Set1-S228, which enhances the stability of transcription-associated Set1 and promotes its binding to chromatin. By controlling the stability of Set1 and its binding at chromatin, Cla4 and the APC/C^{Cdh1} complex regulate the levels of Set1-catalyzed H3K4me3, which then modulates gene transcription, telomere silencing, and chronological life span. In addition to Set1, there are 141 P-box–containing proteins that are co-regulated by Cla4 and the APC/C^{Cdh1} complex. Together, we uncovered a mechanism to regulate Set1 stability within the cell cycle and during gene transcription.

Proteolysis of chromatin modifiers is an important mechanism to maintain the proper chromatin modifications. Histone H3K36 methyltransferase Set2 has a short half-life, and its stability requires its association with RNA Pol II (*7*). Disruption of this interaction results in degradation of Set2 and reduced H3K36 methylation (*7*). Here, we found that Set1 protein is unstable and its protein levels are co-regulated by Cla4 and the APC/C^{Cdh1} complex. As the intracellular Set1 protein level is relatively low, ~135 to 1259 molecules per cell (*32*), we thus speculated that Set1 protein levels might be adjusted to meet cell demand. The strict regulation of Set1 stability within the cell cycle may be beneficial for cells. Set1-catalyzed H3K4me3 has been reported to promote histone gene transcription (*18*). Histone gene transcription is tightly regulated by the cell cycle with their transcription peaked at S phase. The accumulation of excess histones is toxic to cells (*20*). Set1 protein was degraded specifically during G_1 phase, which may avoid synthesis and accumulation of core histones during G_1 phase. Moreover, the PAF complex enhances Cla4-catalyzed Set1-S228 phosphorylation, which ensures that Set1 levels do not exceed the level needed for cotranscriptional histone methylation.

It has been reported that deletion of the N-terminal 780 residues protects Set1 from being degradation (*17*). Yet, the underlying mechanism is unclear. Here, we identified the degron sequence (D-box) within the N-terminal sequence of Set1 and characterized Set1 as a substrate for the APC/C^{Cdh1} complex. Mutation of the D-box stabilized Set1 protein levels and hence increased H3K4me3. Further evidence showed that the E3 ligase APC/C^{Cdh1} complex recognizes the D-box within Set1 N terminus and mediates its proteolysis in G_1 phase and G_2-M phase. By promoting the degradation of Set1, Cdh1 reduces Set1-catalyzed H3K4me3 and is involved in regulation of gene transcription, telomere silencing, and chronological life span.

Cla4 was initially identified to regulate cytokinesis as an effector of Cdc42 (*33*). It was later found to regulate cell polarity during budding (*34*, *35*), vacuole inheritance (*36*), myosin V-dependent organelle transport (*37*), DNA damage response (*38*), the expression of the glycerol biosynthesis enzyme Gpd1 (*39*), etc. Like other protein kinases, Cla4 exerts functions by phosphorylating its substrates, which can regulate their localization and activity. Cla4 has been reported to phosphorylate the vacuole-specific adapter Vac17, which then promotes its ubiquitylation and subsequent degradation (*37*). Here, we identified the HMT Set1 as a target for Cla4. Cla4 phosphorylates Set1-S228, which prevents instead of promotes the ubiquitination and degradation of Set1. Although pyruvate kinase PKM2 has been reported to phosphorylate Bcl2 to prevent the binding of Cul3-based E3 ligase to Bcl2 in mammalian cells (*40*), to the best of our knowledge, there is no report about whether substrate phosphorylation can prevent it from E3-mediated degradation in budding yeast. Our work uncovers a novel function of Cla4 in regulating gene transcription by phosphorylating Set1-S228. It is highly likely that Cla4 regulates gene transcription by interacting with Set1 and the PAF complex. Our ChIP-seq data for Cla4 showed that Cla4 can directly bind 207 genes, among which 68% and 62.5% Cla4-bound genes were co-occupied by Set1 and Paf1, respectively. Set1, Paf1, and Cla4 colocalized at a total of 120 genes. It is hence possible that the PAF complex recruits both Set1 and Cla4 to these 120 genes, where Cla4 efficiently phosphorylates Set1-S228 and stabilizes Set1. We cannot exclude the possibility that the small number of genes occupied by Cla4 may be due to low ChIP efficiency. It is possible that most Cla4 locates in the cytoplasm and only a small amount of Cla4 locates in the nucleus. Another reason could be that the chromatin association of Cla4 may be transient and weak. As Cla4 can phosphorylate Set1-S228 in the absence of nucleosomes (Figs. 2I and 4G), it is possible that Cla4 also phosphorylates free Set1 to stabilize its protein levels. Thus, the global reduction of Set1 protein level may not solely come from 120 colocalized genes.

Our work reveals a relationship between chromatin binding and Set1 stability. The in vitro kinase assay showed that the chromatin association of Set1 facilitates Cla4 to phosphorylate Set1-S228. It is possible that binding to chromatin may lead to conformational change of Set1, which then promotes its phosphorylation by Cla4. Cla4-catalyzed Set1-S228 phosphorylation then antagonizes the effect of APC/C^{Cdh1} complex on Set1 polyubiquitination and proteolysis. Moreover, Cla4-catalyzed Set1-S228 phosphorylation in turn enhances Set1 binding to chromatin, which may increase the time of residency of Set1 complex on chromatin, allowing additional time for Set1 to catalyze H3K4me3 at the 5′-end of genes.

Our results uncover two important roles of the PAF complex in regulating Set1 stability and histone H3K4 methylation. The PAF complex can directly enhance the interaction between Set1 and Cla4 (Fig. 4F), which then facilitates Cla4 to phosphorylate Set1-S228 (Fig. 4G). Therefore, the PAF complex can promote Set1 stability in the absence of chromatin. In the presence of chromatin, the PAF complex can facilitate the binding of Set1 to chromatin (fig. S4K). As the binding of chromatin can increase Set1-S228 phosphorylation (Fig. 4N), it is possible that PAF complex could further promote Set1-S228 phosphorylation and enhance Set1 stability by facilitating Set1 binding to chromatin. Loss of Cdh1 only partly rescued the occupancy of Set1 in *paf1*Δ mutant (fig. S4K), and H3K4me3 was partly restored in *cdh1*Δ *paf1*Δ mutant

(Fig. 5E). It is highly likely that the PAF complex contributes to H3K4 methylation not only by stabilizing Set1 but also by promoting its binding to chromatin. Nonetheless, the PAF complex is not the sole factor that determines Set1 binding to chromatin. Loss of Cdh1 leads to increased Set1, which could bind to chromatin via its interaction with other factors, i.e., RNA Pol II subunit Rpb3 and Spp1 (fig. S4, I and J), which could explain why the loss of Cdh1 can still, but to a lesser extent, increase Set1 binding at chromatin (fig. S4K).

In addition to protecting Set1, Cla4 can potentially phosphorylate a total of 141 proteins and prevent them from degradation by the APC/C^{Cdh1} complex. These proteins contain the P-box (RXpS/TL) that may protect proteins from being recognized and degraded by the APC/C^{Cdh1} complex. These 141 proteins are enriched in cell cycle, meiosis, glycerophospholipid metabolism, and autophagy pathways. By randomly choosing seven proteins from these pathways, we confirmed that their protein levels are regulated by the cell cycle. The co-regulation of protein stability by Cla4 and the APC/C^{Cdh1} complex may connect the above pathways with the cell cycle. It has been reported that the autophagy initiation complex, ULK1-ATG13 complex, is differentially regulated throughout the cell cycle, especially in mitosis, in which both ULK1 and ATG13 are highly phosphorylated by the key cell cycle machinery cyclin-dependent kinase 1 (CDK1)/cyclin B (*41*). CDK1-induced ULK1-ATG13 phosphorylation promotes mitotic autophagy and cell cycle progression. Our data showed that Atg9 is reduced during G_1 phase, and this regulation may be related to Cla4 and the APC/C^{Cdh1} complex, which may directly connect autophagy and the cell cycle.

The budding yeast contains only one Set1 complex to methylate H3K4, which thus serves as an excellent model to study multiple Set1/MLL complex in metazoans (*8*). It remains to be determined whether the mechanism described here is conserved in higher organisms. By analyzing the sequence of Set1 homologs in mammals, including SET1A, SET1B, and MLL1 to MLL4 (*8*), we found that SET1A, SET1B, MLL1, MLL2, and MLL3 were predicted to contain D-box. It is possible that these Set1 homologs could also be degraded by APC/C^{Cdh1}. Recent reports showed that the stability of MLL is regulated at the posttranslational level. MLL undergoes proteolytic cleavage by taspase1 into distinct subunits, MLL(N) and MLL(C), which could then be degraded (*6*, *42*). In addition, MLL1 contains four highly conserved plant homeodomain (PHD) fingers, among which the second PHD finger (PHD2) of MLL1 is an E3 ubiquitin ligase (*43*). Mutation of PHD2 leads to MLL1 stabilization, as well as increased transactivation ability and MLL1 recruitment to the target gene loci (*43*). Blocking MLL1 proteolysis and stabilizing MLL1 may provide a possible approach for clinical therapy of leukemia (*6*). It seems likely that yeast again proves to be a valuable model for understanding all eukaryotic H3K4 methylation in both physiological and pathological conditions.

In summary, we uncovered a mechanism to regulate protein stability by Cla4 and APC/C^{Cdh1}. This mechanism addressed the long-standing question about how Set1 is degraded within the cell cycle and during gene transcription.

MATERIALS AND METHODS

Yeast strains

All yeast strains used in this study are listed in table S2. The yeast mutants were constructed by homologous recombination of PCR fragments according to standard protocols. All yeast strains were verified by colony PCR, DNA sequencing, qRT-PCR, and/or immunoblots before being used for experiments. As there are no commercial antibodies for Cdh1 and Cla4, the deletion of *CDH1* and *CLA4* was validated by PCR and qRT-PCR in fig. S8. For *CDH1* and *CLA4* overexpression strains, they were expressed under the control of a strong (*TEF1*) constitutive promoter.

Antibodies

Antibodies against histone H3 (1: 5000; ab1791) and histone H4 (1:5000; ab10158) were purchased from Abcam; antibodies against Set1 (1:1000; sc-101858) and Rtf1 (1:500; sc-26327) were purchased from Santa Cruz Biotechnology; antibodies against FLAG M2 (1:3000; F1804-1MG) and ubiquitination (FK2, 1:3000; ST1200) were obtained from Sigma-Aldrich; antibodies against H3K4me3 (1:3000; A2357), H3K4me2 (1:5000; A2356), H3K4me1 (1:5000; A2355), His (1:5000; AE003), Alexa Fluor 594–conjugated goat anti-rabbit immunoglobulin G (IgG) (1:500; AS039), and Alexa Fluor 488–conjugated goat anti-mouse IgG (1:500; AS037) were purchased from ABclonal; antibody against glyceraldehyde-3-phosphate dehydrogenase (GAPDH) (1:10000; 10494-1-AP) was obtained from Proteintech; antibody against CBP (1:2000; Abs130593) was purchased from Absin Bioscience Inc.; antibody against Set2 was a gift from H.-N. Du (Wuhan University).

The antibody against Set1-S228p (1:500) was custom-made in ABclonal. The peptide containing Set1-S228p was injected into rabbits, which were approved by the Animal Ethics and Welfare Committee of ABclonal Technology Co. Ltd. The rabbit serum was collected and purified using an affinity column conjugated with nonphosphorylated Set1-S228 peptide to exclude antibodies recognizing nonphosphorylated Set1. Another affinity column conjugated with phosphorylated Set1-S228 peptide was then used to purify the phosphorylated Set1-S228 antibody. The phosphorylated Set1-S228 antibody was eluted and concentrated. The specificity of anti–Set1-S228p was confirmed by dot blots and immunoblots in Fig. 2A and fig. S2A.

Immunoblots

Cells were grown in 5 ml of YPD (yeast extract peptone dextrose) or selective medium as indicated until OD_{600} (optical density at 600 nm) of 0.7 to 1.0 (*22*). Cells were harvested and lysed in buffer containing 0.2 M NaOH. After centrifugation, the protein pellet was resuspended in 200 μl of 2× SDS sample buffer and boiled for 10 min. After centrifugation, the cleared protein samples were separated by 8 to 15% SDS–polyacrylamide gel electrophoresis (PAGE) and transferred to polyvinylidene difluoride (PVDF) membrane. The blots were probed with primary antibodies followed by incubation with horseradish peroxidase–labeled IgG secondary antibodies. The protein bands were visualized using the ECL Chemiluminescence Detection Kit (Bio-Rad, 170-5061) and quantified with ImageJ software (v.1.8.0).

RNA isolation and qRT-PCR

Total RNA was isolated from yeast cells by standard phenol-chloroform extraction procedures as described (*27*). After digestion with DNase I (RNase-free) (Takara, catalog no. 2270A), RNA was quantified by NanoDrop 2000 (Thermo Fisher Scientific). The integrity of RNA was assessed by agarose gel electrophoresis. Total RNA (500 ng) was used for RT-PCR in a 10-μl reaction volume with Reverse Transcriptase Kit (M-MLV) (ZOMANBIO). qPCR was carried out using iTaq Universal SYBR Green Supermix (Bio-Rad, catalog no. 1725121). Primers used for qRT-PCR are described in table S3. We used $2^{-\Delta\Delta Ct}$ to determine the quantity of relative transcription level. The mRNA level of the gene of interest was normalized to that of β-actin.

RNA sequencing

Total RNA was isolated from exponential growing yeast cells by standard phenol-chloroform extraction procedures, and the quality of RNA was examined using Agilent Bioanalyzer according to the manufacturer's instructions. Library construction, sequencing, and bioinformatics analysis were performed by Novogene Co. Ltd. (Beijing, China). There are three biological replicates for WT, Set1-S228A, and Set1-S228E mutants. The differential expression levels of aligned sequences were calculated using significant thresholds set at $\log_2(FC) \leq -0.75$, $\log_2(FC) \geq 0.75$, and $P < 0.05$ (*44*).

Cell synchronization and flow cytometry

Cells were grown in 30 ml of YPD until OD_{600} of 0.7 and then treated with α-factor (10 μg/ml) for 3 hours to arrest cell cycle at G_1. Cells were collected and washed with sterile ddH_2O to remove α-factor. Cells were released to fresh YPD medium and harvested at different time points. For synchronization with other drugs, cells were grown in 30 ml of YPD until OD_{600} = 0.7. The medium was divided into four aliquots, each containing 6 ml of culture. Cells were then individually treated with 10 μM HU, α-factor (10 μg/ml), and 8 μM Noco for 3 hours.

For flow cytometry analysis, cells were collected and fixed in 70% cold ethanol before proceeding to propidium iodide (PI) staining. Fixed cells were washed twice with 50 mM tris pH 7.8 and incubated with RNase A (5 mg/ml) at 24°C for 2 hours. Proteinase K was then added at a final concentration of 1 mg/ml and incubated at 37°C for 2 hours. Cells were washed once with citrate buffer and resuspended at a density of 2×10^6 cells/ml. PI was added to a final concentration of 8 μg/ml followed by 1- to 2-hour incubation and analyzed on an Accuri C6 flow cytometer.

Co-immunoprecipitation

Cells were grown in 200 ml of YPD until OD_{600} of 0.7 to 1.0. Cells were resuspended with H350 buffer (25 mM Hepes-KOH, pH 7.6, 0.5 mM EDTA. 0.02% NP-40, 350 mM KCl, 2 mM $MgCl_2$, 10% glycerol, 1 mM PMSF, 2 μg/ml leupeptin). Cell extract was prepared by vortexing with glass beads. After centrifugation, the supernatant was incubated with anti-FLAG M2 agarose (Sigma) or calmodulin Sepharose beads (GE Healthcare) at 4°C. The beads were washed three times with 3 × 1 ml H350 buffer and boiled in SDS-sample buffer for 10 min. Supernatants from the boiled beads were subjected to SDS-PAGE and immunoblot analysis.

For in vivo Co-IP with histones, the sample was resuspended with HIP buffer (50 mM tris, pH 7.5, 150 mM NaCl, 1.5 mM MgAc, 10% glycerol, 0.15% NP-40, 1 mM PMSF, 2 μg/ml leupeptin). Cell extract was prepared by vortexing with glass beads. The chromatin in the sample was further fragmented by sonication followed by digestion with micrococcal nuclease (MNase) for 1 hour. The sample was centrifuged at 15,000 rpm at 4°C for 15 min. The supernatant was incubated with anti-FLAG M2 agarose (Sigma) at 4°C for 8 hours. The beads were washed three times with HIP buffer and boiled in SDS-sample buffer for 10 min. Supernatants from the boiled beads were subjected to SDS-PAGE and immunoblots.

Protein expression and purification

CDH1 and *SET1* genes were cloned into the pCold-His vector and expressed in BL21(DE3). Proteins were purified using the Ni-NTA Agarose (QIAGEN) as described (*45*). Ctr9-TAP was purified by tandem affinity purification (TAP) from yeast cells as described (*46*).

In vitro kinase assay

Set1 peptide (20 ng) (CRNS228LILLP) or purified recombinant Set1-His (20 μg) was mixed with 10 μg of purified recombinant Cla4-His in 2× kinase buffer (100 mM tris-HCl, pH 7.4, 100 mM $MgCl_2$, 10 mM ATP, 0.2 μM PMSF, 1 mM Na_3VO_4, 5% glycerol) at 30°C for 0 to 1 hour. The reaction was quenched by adding 2× SDS-PAGE loading buffer and incubated at 95°C for 10 min followed by dot blots or immunoblots.

Mass spectrometry analysis

Cla4-FLAG and FLAG-Set1 cells were grown in 4 liters of YPD medium to an OD_{600} of 1.0 to 1.5, collected, and snap-frozen in liquid nitrogen (*44*). Thawed cell pellets were lysed with glass beads by using a Biospec bead beater (30 s ON, 90 s OFF) for 70 min in H350 buffer (25 mM Hepes-KOH, pH 7.6, 0.5 mM EDTA, 0.02% NP-40, 350 mM KCl, 2 mM $MgCl_2$, 10% glycerol, 1 mM PMSF, 2 μg/ml leupeptin, 50 mM NaF, 1 mM Na_3VO_4). The lysate was cleared by centrifugation at 45,000 rpm at 4°C for 1.5 hours, and the supernatant was incubated with anti-FLAG M2 affinity gel (Sigma) at 4°C for 8 hours. The beads were washed extensively in H350 buffer, and the immunoprecipitated proteins were disulfide-reduced by 25 mM dithiothreitol at 37°C for 40 min. Cysteines were alkylated by 50 mM iodoacetamide in the dark for 30 min. The immunoprecipitated proteins were digested overnight with sequencing-grade trypsin (Promega) at 37°C and desalted using C18 columns (Thermo Fisher Scientific) and lyophilized. The dried peptides were reconstituted in 0.1% formic acid (FA) and loaded onto an Acclaim PepMap 100 C18 LC column (Thermo Fisher Scientific) using a Thermo Easy nLC 1000 LC system (Thermo Fisher Scientific) connected to QEHF Orbitrap mass spectrometer (Thermo Fisher Scientific). The raw mass spectrometry data were searched against the *Saccharomyces cerevisiae* proteome database from UniProt (https://www.uniprot.org/proteomes/UP000002311) using Sequest HT, MS Amanda, and ptmRS algorithms in Proteome Discoverer 2.3 (Thermo Fisher Scientific).

Molecular docking

The crystal structure of Cla4-homolog Pak4 was obtained from the Protein Data Bank (PDBID: 2X4Z). To visualize the docked conformation, water molecules and glycerol ligands were removed in the PyMoL molecular graphics system. The structure of Set1 peptides

(226-RNSL-229) was generated using I-TASSER protein Structure and Function Prediction web server (http://zhanglab.ccmb.med.umich.edu/I-TASSER/). Molecular docking simulation of Pak4 and Set1 peptides was performed with the AutoDock Vina.

ITC assay

The thermodynamic parameters for the binding of Cdh1 to Set1 peptides were measured with ITC assays using the Nano ITC (TA Instruments) at 25°C as described (*46*). For all experiments, the initial injection of 0.5 μl of Set1 peptide solution was discarded to eliminate the effect of titrant diffusion across the syringe tip during the equilibration process, and each dataset consists of 20 injections of 2.5 μl each of 2 mM Set1-S228 peptide or Set1-S228p peptide into a sample cell containing 500 μl of 0.25 mM purified Cdh1. The heat of dilution was negligible in all cases. The dissociation constant (K_d) and other thermodynamic parameters were determined by fitting the integrated titration data using the independent model implemented in Nanoanalyzer software (v.3.7.5).

ChIP assay

Yeast cells were grown in 200 ml of YPD medium at 30°C until OD_{600} of 1.0 to 1.5. The samples were crosslinked with 1% formaldehyde, and the crosslinking was quenched by adding 10 ml of 2.5 M glycine as described (*44*). After centrifugation, cells were washed with cold washing buffer (tris-buffered saline + 1 mM PMSF), lysed with glass beads in FA-SDS lysis buffer (40 mM Hepes-KOH, pH 7.5, 1 mM EDTA, pH 8.0, 0.1% SDS, 1% Triton X-100, 0.1% Na deoxycholate, 1 mM PMSF, 2 μg/ml leupeptin, 1 μg/ml pepstatin A, protease inhibitor cocktail). Chromatin was sonicated to an average size of ~500 bp and then subjected to immunoprecipitation with anti-FLAG M2 antibody (5 μl, F1804, Sigma), anti-H3 (2 μl; ab1791, Abcam), and anti-H3K4me3 (2 μl; A2369, ABclonal) prebound to Protein G Dynabeads (Invitrogen) at 4°C overnight. The beads were then washed successively with FA lysis buffer, FA buffer + 1 M NaCl, FA buffer + 0.5 M NaCl, TEL buffer (10 mM tris, pH 8.0, 1 mM EDTA, 0.25 M LiCl, 1% NP-40, 1% Na deoxycholate), and TE (10 mM tris, pH 7.4, 1 mM EDTA). The eluted DNA/protein complexes were treated with 2 μl of proteinase K (10 μg/μl) to remove proteins at 55°C for 1 hour and then treated at 65°C overnight. The libraries were constructed and sequenced on an Illumina platform (*47*). Reads were aligned to yeast genome sacCer3 from UCSC using bowtie2 version 2.1.0 with parameter -k 1. Telomere repeated sequences were excluded for further analysis. Data were read into R (3.1.0) for further analysis. Peaks were called using MACS2 (v.2.1.1, macs2 callpeak) with parameter -t -c -g 1.2e7 -n -B -q 0.01 --nomodel. Peak annotation was performed on a website service (https://manticore.niehs.nih.gov/pavis2/). Tracks were smoothed by deepTools2 (v.2.0) and visualized by IGV software (v.2.0) with a reference genome of *S. cerevisiae* (sacCer3).

GAL1 transcription memory assay

Cells were grown in 20 ml of YPD until OD_{600} of 0.7. Cells were collected by centrifugation in 4000 rpm at 4°C for 3 min. The sample was washed by YP medium for three times, resuspended in 20 ml of YP medium, and divided into two aliquots, which were individually added 2% glucose and 2% galactose and incubated at 37°C for 2.5 hours, which were called initial induction. After that, cells were washed twice with sterilized ddH_2O, released into YPD medium, and incubated at 37°C for 1 hour. After that, cells were washed twice with sterilized water and divided into two aliquots for re-induction. One aliquot was treated with 2% glucose, and the other aliquot was treated with 2% galactose. Cells were collected at different time points and snap-frozen in liquid nitrogen immediately.

Statistics and reproducibility

Representative results of at least two biological independent experiments were performed in all of the figure panels. The two-sided Student's *t* test was used for comparison between two groups, and a *P* value of <0.05 was considered statistically significant. $^*P < 0.05$, $^{**}P < 0.01$, $^{***}P < 0.001$. For all error bars, data are mean ± SE.

Supplementary Materials

This PDF file includes:

Figs. S1 to S8
Tables S1 to S3

REFERENCES AND NOTES

1. T. Kouzarides, Chromatin modifications and their function. *Cell* **128**, 693–705 (2007).
2. W. A. Flavahan, E. Gaskell, B. E. Bernstein, Epigenetic plasticity and the hallmarks of cancer. *Science* **357**, (2017).
3. H. Yuan, Y. Han, X. Wang, N. Li, Q. Liu, Y. Yin, H. Wang, L. Pan, L. Li, K. Song, T. Qiu, Q. Pan, Q. Chen, G. Zhang, Y. Zang, M. Tan, J. Zhang, Q. Li, X. Wang, J. Jiang, J. Qin, SETD2 restricts prostate cancer metastasis by integrating EZH2 and AMPK signaling pathways. *Cancer Cell* **38**, 350–365.e7 (2020).
4. R. S. Derr, A. Q. van Hoesel, A. Benard, I. J. Goossens-Beumer, A. Sajet, N. G. Dekker-Ensink, E. M. de Kruijf, E. Bastiaannet, V. T. H. B. M. Smit, C. J. H. van de Velde, P. J. K. Kuppen, High nuclear expression levels of histone-modifying enzymes LSD1, HDAC2 and SIRT1 in tumor cells correlate with decreased survival and increased relapse in breast cancer patients. *BMC Cancer* **14**, 604 (2014).
5. X. Cheng, Y. Hao, W. Shu, M. Zhao, C. Zhao, Y. Wu, X. Peng, P. Yao, D. Xiao, G. Qing, Z. Pan, L. Yin, D. Hu, H. N. du, Cell cycle-dependent degradation of the methyltransferase SETD3 attenuates cell proliferation and liver tumorigenesis. *J. Biol. Chem.* **292**, 9022–9033 (2017).
6. Z. Zhao, L. Wang, A. G. Volk, N. W. Birch, K. L. Stoltz, E. T. Bartom, S. A. Marshall, E. J. Rendleman, C. M. Nestler, J. Shilati, G. E. Schiltz, J. D. Crispino, A. Shilatifard, Regulation of MLL/COMPASS stability through its proteolytic cleavage by taspase1 as a possible approach for clinical therapy of leukemia. *Genes Dev.* **33**, 61–74 (2019).
7. S. M. Fuchs, K. O. Kizer, H. Braberg, N. J. Krogan, B. D. Strahl, RNA polymerase II carboxyl-terminal domain phosphorylation regulates protein stability of the Set2 methyltransferase and histone H3 di- and trimethylation at lysine 36. *J. Biol. Chem.* **287**, 3249–3256 (2012).
8. A. Shilatifard, The COMPASS family of histone H3K4 methylases: Mechanisms of regulation in development and disease pathogenesis. *Annu. Rev. Biochem.* **81**, 65–95 (2012).
9. D. Faucher, R. J. Wellinger, Methylated H3K4, a transcription-associated histone modification, is involved in the DNA damage response pathway. *PLOS Genet.* **6**, e1001082 (2010).
10. J. A. Daniel, A. Nussenzweig, Roles for histone H3K4 methyltransferase activities during immunoglobulin class-switch recombination. *Biochim. Biophys. Acta* **1819**, 733–738 (2012).
11. B. A. Nacev, L. Feng, J. D. Bagert, A. E. Lemiesz, J. J. Gao, A. A. Soshnev, R. Kundra, N. Schultz, T. W. Muir, C. D. Allis, The expanding landscape of 'oncohistone' mutations in human cancers. *Nature* **567**, 473–478 (2019).
12. A. K. Andersson, J. Ma, J. Wang, X. Chen, A. L. Gedman, J. Dang, J. Nakitandwe, L. Holmfeldt, M. Parker, J. Easton, R. Huether, R. Kriwacki, M. Rusch, G. Wu, Y. Li, H. Mulder, S. Raimondi, S. Pounds, G. Kang, L. Shi, J. Becksfort, P. Gupta, D. Payne-Turner, B. Vadodaria, K. Boggs, D. Yergeau, J. Manne, G. Song, M. Edmonson, P. Nagahawatte, L. Wei, C. Cheng, D. Pei, R. Sutton, N. C. Venn, A. Chetcuti, A. Rush, D. Catchpoole, J. Heldrup, T. Fioretos, C. Lu, L. Ding, C.-H. Pui, S. Shurtleff, C. G. Mullighan, E. R. Mardis, R. K. Wilson, T. A. Gruber, J. Zhang, J. R. Downing; St. Jude Children's Research Hospital–Washington University Pediatric Cancer Genome Project, The landscape of somatic mutations in infant MLL-rearranged acute lymphoblastic leukemias. *Nat. Genet.* **47**, 330–337 (2015).
13. H. H. Ng, F. Robert, R. A. Young, K. Struhl, Targeted recruitment of Set1 histone methylase by elongating Pol II provides a localized mark and memory of recent transcriptional activity. *Mol. Cell* **11**, 709–719 (2003).

14. N. J. Krogan, J. Dover, A. Wood, J. Schneider, J. Heidt, M. A. Boateng, K. Dean, O. W. Ryan, A. Golshani, M. Johnston, J. F. Greenblatt, A. Shilatifard, The Paf1 complex is required for histone H3 methylation by COMPASS and Dot1p: Linking transcriptional elongation to histone methylation. *Mol. Cell* **11**, 721–729 (2003).
15. C. L. Mueller, J. A. Jaehning, Ctr9, Rtf1, and Leo1 are components of the Paf1/RNA polymerase II complex. *Mol. Cell. Biol.* **22**, 1971–1980 (2002).
16. X. Gong, Q. Yu, K. Duan, Y. Tong, X. Zhang, Q. Mei, L. Lu, X. Yu, S. Li, Histone acetyltransferase Gcn5 regulates gene expression by promoting the transcription of histone methyltransferase SET1. *Biochim. Biophys. Acta Gene Regul. Mech.* **1863**, 194603 (2020).
17. L. M. Soares, M. Radman-Livaja, S. G. Lin, O. J. Rando, S. Buratowski, Feedback control of Set1 protein levels is important for proper H3K4 methylation patterns. *Cell Rep.* **6**, 961–972 (2014).
18. Q. Mei, C. Xu, M. Gogol, J. Tang, W. Chen, X. Yu, J. L. Workman, S. Li, Set1-catalyzed H3K4 trimethylation antagonizes the HIR/Asf1/Rtt106 repressor complex to promote histone gene expression and chronological life span. *Nucleic Acids Res.* **47**, 3434–3449 (2019).
19. Q. Mei, Q. Yu, X. Li, J. Chen, X. Yu, Regulation of telomere silencing by the core histones-autophagy-Sir2 axis. *Life Sci. Alliance* **6**, e202201614 (2023).
20. Q. Mei, J. Huang, W. Chen, J. Tang, C. Xu, Q. Yu, Y. Cheng, L. Ma, X. Yu, S. Li, Regulation of DNA replication-coupled histone gene expression. *Oncotarget* **8**, 95005–95022 (2017).
21. I. Dikic, Proteasomal and autophagic degradation systems. *Annu. Rev. Biochem.* **86**, 193–224 (2017).
22. S. Zhang, X. Yu, Y. Zhang, X. Xue, Q. Yu, Z. Zha, M. Gogol, J. L. Workman, S. Li, Metabolic regulation of telomere silencing by SESAME complex-catalyzed H3T11 phosphorylation. *Nat. Commun.* **12**, 594 (2021).
23. L. Qin, D. S. Guimaraes, M. Melesse, M. C. Hall, Substrate recognition by the Cdh1 destruction box receptor is a general requirement for APC/CCdh1-mediated proteolysis. *J. Biol. Chem.* **291**, 15564–15574 (2016).
24. E. Choi, J. M. Dial, D. E. Jeong, M. C. Hall, Unique D box and KEN box sequences limit ubiquitination of Acm1 and promote pseudosubstrate inhibition of the anaphase-promoting complex. *J. Biol. Chem.* **283**, 23701–23710 (2008).
25. J. A. Pesin, T. L. Orr-Weaver, Regulation of APC/C activators in mitosis and meiosis. *Annu. Rev. Cell Dev. Biol.* **24**, 475–499 (2008).
26. J. Mok, P. M. Kim, H. Y. K. Lam, S. Piccirillo, X. Zhou, G. R. Jeschke, D. L. Sheridan, S. A. Parker, V. Desai, M. Jwa, E. Cameroni, H. Niu, M. Good, A. Remenyi, J.-L. N. Ma, Y.-J. Sheu, H. E. Sassi, R. Sopko, C. S. M. Chan, C. De Virgilio, N. M. Hollingsworth, W. A. Lim, D. F. Stern, B. Stillman, B. J. Andrews, M. B. Gerstein, M. Snyder, B. E. Turk, Deciphering protein kinase specificity through large-scale analysis of yeast phosphorylation site motifs. *Sci. Signal.* **3**, ra12 (2010).
27. X. Li, Q. Mei, Q. Yu, M. Wang, F. He, D. Xiao, H. Liu, F. Ge, X. Yu, S. Li, The TORC1 activates Rpd3L complex to deacetylate Ino80 and H2A.Z and repress autophagy. *Sci. Adv.* **9**, eade8312 (2023).
28. H. J. Bae, M. Dubarry, J. Jeon, L. M. Soares, C. Dargemont, J. Kim, V. Geli, S. Buratowski, The Set1 N-terminal domain and Swd2 interact with RNA polymerase II CTD to recruit COMPASS. *Nat. Commun.* **11**, 2181 (2020).
29. A. Kirmizis, H. Santos-Rosa, C. J. Penkett, M. A. Singer, M. Vermeulen, M. Mann, J. Bähler, R. D. Green, T. Kouzarides, Arginine methylation at histone H3R2 controls deposition of H3K4 trimethylation. *Nature* **449**, 928–932 (2007).
30. B. O. Zhou, J. Q. Zhou, Recent transcription-induced histone H3 lysine 4 (H3K4) methylation inhibits gene reactivation. *J. Biol. Chem.* **286**, 34770–34776 (2011).
31. I. M. Fingerman, C. L. Wu, B. D. Wilson, S. D. Briggs, Global loss of Set1-mediated H3 Lys4 trimethylation is associated with silencing defects in Saccharomyces cerevisiae. *J. Biol. Chem.* **280**, 28761–28765 (2005).
32. M. Breker, M. Gymrek, M. Schuldiner, A novel single-cell screening platform reveals proteome plasticity during yeast stress responses. *J. Cell Biol.* **200**, 839–850 (2013).
33. J. Kadota, T. Yamamoto, S. Yoshiuchi, E. Bi, K. Tanaka, Septin ring assembly requires concerted action of polarisome components, a PAK kinase Cla4p, and the actin cytoskeleton in Saccharomyces cerevisiae. *Mol. Biol. Cell* **15**, 5329–5345 (2004).
34. L. Leveleki, M. Mahlert, B. Sandrock, M. Bolker, The PAK family kinase Cla4 is required for budding and morphogenesis in Ustilago maydis. *Mol. Microbiol.* **54**, 396–406 (2004).
35. M. Geymonat, A. Spanos, S. Jensen, S. G. Sedgwick, Phosphorylation of Lte1 by Cdk prevents polarized growth during mitotic arrest in S. cerevisiae. *J. Cell Biol.* **191**, 1097–1112 (2010).
36. C. R. Bartholomew, C. F. Hardy, p21-activated kinases Cla4 and Ste20 regulate vacuole inheritance in *Saccharomyces cerevisiae*. *Eukaryot. Cell* **8**, 560–572 (2009).
37. R. G. Yau, S. Wong, L. S. Weisman, Spatial regulation of organelle release from myosin V transport by p21-activated kinases. *J. Cell Biol.* **216**, 1557–1566 (2017).
38. G. Millan-Zambrano, H. Santos-Rosa, F. Puddu, S. C. Robson, S. P. Jackson, T. Kouzarides, Phosphorylation of histone H4T80 triggers DNA damage checkpoint recovery. *Mol. Cell* **72**, 625–635.e4 (2018).
39. I. M. Joshua, T. Hofken, Ste20 and Cla4 modulate the expression of the glycerol biosynthesis enzyme Gpd1 by a novel MAPK-independent pathway. *Biochem. Biophys. Res. Commun.* **517**, 611–616 (2019).
40. J. Liang, R. Cao, X. Wang, Y. Zhang, P. Wang, H. Gao, C. Li, F. Yang, R. Zeng, P. Wei, D. Li, W. Li, W. Yang, Mitochondrial PKM2 regulates oxidative stress-induced apoptosis by stabilizing Bcl2. *Cell Res.* **27**, 329–351 (2017).
41. Z. Li, X. Tian, X. Ji, J. Wang, H. Chen, D. Wang, X. Zhang, ULK1-ATG13 and their mitotic phospho-regulation by CDK1 connect autophagy to cell cycle. *PLOS Biol.* **18**, e3000288 (2020).
42. A. Yokoyama, F. Ficara, M. J. Murphy, C. Meisel, A. Naresh, I. Kitabayashi, M. L. Cleary, Proteolytically cleaved MLL subunits are susceptible to distinct degradation pathways. *J. Cell Sci.* **124**, 2208–2219 (2011).
43. J. Wang, A. G. Muntean, L. Wu, J. L. Hess, A subset of mixed lineage leukemia proteins has plant homeodomain (PHD)-mediated E3 ligase activity. *J. Biol. Chem.* **287**, 43410–43416 (2012).
44. Q. Yu, X. Gong, Y. Tong, M. Wang, K. Duan, X. Zhang, F. Ge, X. Yu, S. Li, Phosphorylation of Jhd2 by the Ras-cAMP-PKA(Tpk2) pathway regulates histone modifications and autophagy. *Nat. Commun.* **13**, 5675 (2022).
45. W. Chen, X. Yu, Y. Wu, J. Tang, Q. Yu, X. Lv, Z. Zha, B. Hu, X. Li, J. Chen, L. Ma, J. L. Workman, S. Li, The SESAME complex regulates cell senescence through the generation of acetyl-CoA. *Nat. Metab.* **3**, 983–1000 (2021).
46. J. Huang, W. Dai, D. Xiao, Q. Xiong, C. Liu, J. Hu, F. Ge, X. Yu, S. Li, Acetylation-dependent SAGA complex dimerization promotes nucleosome acetylation and gene transcription. *Nat. Struct. Mol. Biol.* **29**, 261–273 (2022).
47. F. He, Q. Yu, M. Wang, R. Wang, X. Gong, F. Ge, X. Yu, S. Li, SESAME-catalyzed H3T11 phosphorylation inhibits Dot1-catalyzed H3K79me3 to regulate autophagy and telomere silencing. *Nat. Commun.* **13**, 7526 (2022).

Acknowledgments: We thank H.-N. Du (Wuhan University) for providing us the antibody against Set2. We thank the Li laboratory members for discussion. **Funding:** This work was supported by funding from the National Natural Science Foundation of China (31970578 to S.L.), the Natural Science Foundation of Hubei Province (2021CFA013 to S.L.), the State Key Laboratory of Cardiovascular Disease, Fuwai Hospital, Chinese Academy of Medical Sciences (2022ZD-01), and the Key Science and Technology Innovation Project of Hubei Province (2021BAD001). **Author contributions:** Conceptualization: X.Y. and S.L. Methodology: X.G., S.W., Q.Y., and F.G. Investigation: X.G., S.W., and M.W. Visualization: X.G. Supervision: X.Y. and S.L. Writing—original draft: X.Y. and S.L. Writing—review and editing: S.L., X.Y., and S.W. **Competing interests:** The authors declare that they have no competing interests. **Data and materials availability:** All data needed to evaluate the conclusions in the paper are present in the paper and/or the Supplementary Materials. The accession code for ChIP-seq of H3K4me3 and Cla4 generated in this study has been deposited in the GEO database under accession number GSE229516. The accession number for ChIP-seq of WT Set1, Set1-S228A, and Set1-S228E in *cdh1*Δ background in this paper is GSE239705. The accession number for the raw RNA-seq dataset (WT Set1, Set1-S228A, and Set1-S228E) in this paper is GSE208095. The ChIP-seq data for Set1 and Paf1 are available in the GEO database under accession numbers GSE72972 and GSE147927, respectively. The mass spectrometry proteomics data have been deposited to the ProteomeXchange Consortium with the dataset identifier PXD042010. The plasmids and strains can be provided by corresponding authors pending a completed material transfer agreement.

Submitted 15 May 2023
Accepted 30 August 2023
Published 29 September 2023
10.1126/sciadv.adi7238